Arabidopsis ABCG34 contributes to defense against necrotrophic pathogens by mediating the secretion of camalexin

Khare, Deepa ; Choi, Hyunju ; Huh, Sung Un ; Bassin, Barbara ; Kim, Jeongsik ; Martinoia, Enrico ; Sohn, Kee Hoon ; Paek, Kyung-Hee ; Lee, Youngsook

Abstract: Plant pathogens cause huge yield losses. Plant defense often depends on toxic secondary metabolites that inhibit pathogen growth. Because most secondary metabolites are also toxic to the plant, specific transporters are needed to deliver them to the pathogens. To identify the transporters that function in plant defense, we screened Arabidopsis thaliana mutants of full-size ABCG transporters for hypersensitivity to sclareol, an antifungal compound. We found that atabcg34 mutants were hypersensitive to sclareol and to the necrotrophic fungi Alternaria brassicicola and Botrytis cinereaAtABCG34 expression was induced by Abrassicicola inoculation as well as by methyl-jasmonate, a defense-related phytohormone, and AtABCG34 was polarly localized at the external face of the plasma membrane of epidermal cells of leaves and roots. atabcg34 mutants secreted less camalexin, a major phytoalexin in Athaliana, whereas plants overexpressing AtABCG34 secreted more camalexin to the leaf surface and were more resistant to the pathogen. When treated with exogenous camalexin, atabcg34 mutants exhibited hypersensitivity, whereas BY2 cells expressing AtABCG34 exhibited improved resistance. Analyses of natural Arabidopsis accessions revealed that AtABCG34 contributes to the disease resistance in naturally occurring genetic variants, albeit to a small extent. Together, our data suggest that AtABCG34 mediates camalexin secretion to the leaf surface and thereby prevents Abrassicicola infection.

DOI: https://doi.org/10.1073/pnas.1702259114

Originally published at:
Khare, Deepa; Choi, Hyunju; Huh, Sung Un; Bassin, Barbara; Kim, Jeongsik; Martinoia, Enrico; Sohn, Kee Hoon; Paek, Kyung-Hee; Lee, Youngsook (2017). Arabidopsis ABCG34 contributes to defense against necrotrophic pathogens by mediating the secretion of camalexin. Proceedings of the National Academy of Sciences of the United States of America, 114(28):E5712-E5720.
DOI: https://doi.org/10.1073/pnas.1702259114

BIOLOGICAL SCIENCES, Plant Biology

Arabidopsis ABCG34 contributes to defense against necrotrophic pathogens by mediating the secretion of camalexin

Deepa Khare[a], Hyunju Choi[a], Sung Un Huh[b,c], Barbara Bassin[d], Jeongsik Kim[e], Enrico Martinoia[d], Kee Hoon Sohn[a,f], Kyung-Hee Paek[b,1], Youngsook Lee[a,g,1,2]

[a]Department of Life Sciences, POSTECH, Pohang, 37673, Republic of Korea, [b]Department of Life Sciences, Korea University, 145 Anam-ro, Seongbuk-gu, Seoul, 02841, Republic of Korea, [c]The Sainsbury Laboratory, Norwich Research Park, Colney Lane, Norwich, NR4 7UH, UK, [d]Department of Plant and Microbial Biology, University of Zurich, Zurich, 8008 Zurich, Switzerland, [e]Center for Plant Aging Research, Institute for Basic Science (IBS), Daegu, 42988, Republic of Korea, [f]School of Interdisciplinary Bioscience and Bioengineering, POSTECH, Pohang, 37673, Republic of Korea, [g]Division of Integrative Bioscience and Biotechnology, POSTECH, Pohang, 37673, Republic of Korea

[1]These authors contributed equally to this work.

[2]Corresponding author: Youngsook Lee

Tel: +82542792296

Email: ylee@postech.ac.kr

Keywords: AtABCG34, ABC transporters, pathogens, camalexin, *A. brassicicola*, *B. cinerea*

Abstract

Plant pathogens cause huge yield losses. Plant defense often depends on toxic secondary metabolites that inhibit pathogen growth. Since most secondary metabolites are toxic to the plant, too, specific transporters are needed to deliver them to the pathogens. To identify transporters that function in plant defense, we screened *Arabidopsis thaliana* mutants of full-size ABCG transporters for hypersensitivity to sclareol, an antifungal compound. We found that *atabcg34* mutants were hypersensitive to sclareol and the necrotrophic fungi *Alternaria brassicicola* and *Botrytis cinerea*. *AtABCG34* expression was induced by *A. brassicicola* inoculation as well as by methyl-jasmonate, a defense-related phytohormone, and AtABCG34 was polarly localized at the external face of the plasma membrane of epidermal cells of leaves and roots. *atabcg34* mutants secreted less camalexin, a major phytoalexin in *A. thaliana*, while AtABCG34-overexpressing plants secreted more camalexin to the leaf surface, and were more resistant to the pathogen. When treated with exogenous camalexin, *atabcg34* mutants exhibited hypersensitivity, whereas BY2 cells expressing AtABCG34 exhibited improved resistance. Analyses of natural *Arabidopsis* accessions revealed that AtABCG34 contributes to the disease resistance in naturally occurring genetic variants, albeit to a small extent. Together, our data suggest that AtABCG34 mediates camalexin secretion to the leaf surface, and thereby prevents *A. brassicicola* infection.

Significance statement

Alternaria brassicicola infection causes dark spots on the leaves of most *Brassica* species, reducing the yield of economically-important oilseed crops. In

response to *A. brassicicola* infection, *Arabidopsis thaliana* and other Brassicaceae produce and secrete camalexin, a major phytoalexin imparting resistance to *A. brassicicola.* Since camalexin is toxic to the plant itself, specific transporters are needed for secretion. In this work, we have shown that the ABC transporter ABCG34 mediates the secretion of camalexin from the epidermal cells to the surface of leaves, and thereby confers resistance to *A. brassicicola* infection. This work establishes a complete picture of a plant defense system, consisting of a toxic secondary metabolite, its transporter, and the disease phenotype caused by an economically important pathogen.

/Body

Introduction

Plants are exposed to a multitude of pathogens, but they usually resist infection using their unique defense systems and compounds, including secondary metabolites produced either constitutively (phytoanticipins) or in response to pathogen attack (phytoalexins). Plants produce tens of thousands of secondary metabolites, which are classified into phenolics, terpenoids, alkaloids, glucosinolates, cyanogenic glucosides and betanins. Secondary metabolites are either secreted from the infected cells and their surrounding cells after pathogen attack, or released, hydrolyzed, and become toxic when the cells are destroyed by pathogens (1), thus inhibiting pathogen growth on the plant. Many secondary metabolites are dangerous to plants, too, because of their toxicity to cellular metabolism. To avoid self toxicity, plants either secrete these compounds to the leaf surface or sequester them into the vacuole, a compartment with low metabolic activity. In both cases, specific transporters are required either to deliver the secondary metabolites to where the pathogens are located or to store them as weapons against pathogen attack.

Several full-size ABCG transporters are involved in the transport of secondary

metabolites. *Nicotiana plumbaginifolia* PDR1/ABC1 and *Nicotiana tabacum* PDR1 are induced by jasmonate, a defense-related hormone, highly expressed in the leaf epidermal cells and trichomes, and transport sclareol, a diterpene alcohol secreted by *Nicotiana* species in response to pathogen attack (2, 3, 4). Two functionally redundant *Nicotiana benthamiana* full-size ABCG transporters, NbABCG1 and NbABCG2, are essential for resistance to *Phytophthora infestans*. Mutants with defects in these two ABCG transporters export much less capsidiol than do the corresponding wild-type plants, indicating that these transporters transport capsidiol (5). NtABCG5/NtPDR5 is induced by insect herbivory, and absence of this transporter decreases resistance to insects, indicating that it is involved in the transport of a hitherto unidentified insecticidal compound (6). Absence of PhPDR2 increases insect herbivory in *Petunia hybrida* leaves and decreases concentrations of the insecticidal steroid petuniasterone (7). CrTPT2 secretes catharanthine to the leaf surface and expresses at the plasma membrane of *Catharanthus roseus* (8). Lr34, an ABCG transporter in *Triticum aestivum* (wheat), is one of the few durable resistance genes that protect the plant from multiple pathogens: namely *Puccinia triticina* and *Puccinia striiformis* which cause leaf rust and *Blumeria graminis* which causes powdery mildew (9). Furthermore, Lr34 confers resistance to multiple isolates of *Magnaporthe oryzae* when heterologously expressed in *Oryza sativa* (rice) (10). Thus it is a promising candidate ABC transporter to use in crop plants to improve disease resistance to a broad spectrum of pathogens. However, the substrate transported by Lr34 is still unknown.

Among the 129 ABC proteins present in *Arabidopsis thaliana*, only two have been implicated in the defense response. PDR8/ABCG36/PEN3, which is localized at the plasma membrane, recruited to infection sites (11), and involved in glucosinolate-

dependent pathogen defense at the contact site (12), blocks the penetration of non-host fungal pathogens (13). Recently, a report suggested that this protein transports 4-O-β-D-glucosyl-indol-3-yl formamide (4OGlcI3F) (14); however, this remains to be proven. *atabcg40/pdr12* mutants exhibit sensitivity to sclareol and *AtABCG40/PDR12* is induced by pathogen inoculation (15). However, sclareol is not likely the natural substrate of AtABCG40, because it is not synthesized in *A. thaliana.* Thus, AtABCG40 might transport chemicals similar to sclareol that are produced by *A. thaliana* in response to pathogen attack.

We hypothesized that additional ABCG transporters are involved in pathogen defense, since 1) the transcript levels of many additional full-size ABCG transporters have been reported to be up-regulated in plants exposed to pathogens (16, 17), and 2) pathogen defense is often mediated by secondary metabolites, many of which are transported by ABC transporters (18). To identify such additional ABCG transporters involved in plant defense against pathogens, we screened *A. thaliana* T-DNA insertion mutants of full-size *ABCG* genes for altered sensitivity to the secondary metabolite sclareol, since sclareol hypersensitivity might provide a clue as to which ABCG proteins are involved in secondary metabolite transport. Having established that *atabcg34* is hypersensitive to sclareol, we analyzed the function of AtABCG34 in relation to transport of secondary metabolites implicated in pathogen defense.

Results

atabcg34 mutants exhibit hypersensitivity to sclareol

To identify new transporters involved in pathogen defense, we exposed 13 of the 15 full-

length *A. thaliana abcg* transporter mutants (except *atabcg42* and *atabcg43*, as knockout mutants of these genes were not available at the time of screening) to a toxic concentration of sclareol (65 µM). Among the mutants, *atabcg34-1* (*ko-1;* SAIL_5_G10) and *atabcg34-2* (*ko-2*; SALK_036087; Fig. S1) exhibited the strongest reduction of both fresh weight and root length in sclareol containing medium (Fig. 1 A, C and D). Expression of the genomic fragment of *AtABCG34* (*ABCG34pro:sGFP:ABCG34;* gDNA) rescued the mutants from sensitivity to sclareol; both fresh weight and root length of the complementation lines recovered to levels similar to those of wild-type plants in ½ MS medium supplemented with 65 µM sclareol (Fig. 1 B-D for *ko-1*, Fig. S2 for *ko-2*). Interestingly, although AtABCG39 is the closest relative of AtABCG34 among the full-size ABCG members (Fig. S3A), and its amino acid sequence is 89% identical with that of AtABCG34, the *atabcg39* mutant was not sensitive to sclareol (Fig. S3 B and C).

AtABCG34 contributes to plant defense against necrotrophic fungi

Since sclareol is known to restrict fungal growth (19, 20), we speculated that AtABCG34 might be involved in defense against fungal pathogens. We evaluated this possibility by inoculating the *atabcg34* mutants (*ko-1* and *ko-2*) with two different necrotrophic fungi, *B. cinerea* and *A. brassicicola*. Whereas the wild-type leaves inoculated with the two pathogens became necrotic only at the inoculation sites, the mutant leaves exhibited much more extensive necrotic areas upon infection with *A. brassicicola* (Fig. 2 A and B) or *B. cinerea* (Fig. S4A; left panel), which suggested that the mutants were hypersensitive to both necrotrophic fungal pathogens. Quantification of the pathogen growth confirmed that the *atabcg34* mutants were hypersensitive to the fungal pathogens. *A. brassicicola* growth, quantified using quantitative-PCR of *A. brassicicola cutinase A*

genomic DNA relative to *A. thaliana α-shaggy kinase* genomic DNA, was higher in the mutant leaves than in those of the wild type or the complementation lines (Fig. 2C). *B. cinerea* growth, measured by counting spore numbers (Fig. S4A; right), was also higher in the mutant leaves than in the wild-type leaves. By contrast, the mutants' response to a bacterial pathogen, *Pseudomonas syringae pv. tomato* DC3000 (*Pst* DC3000), was similar to that of the wild type (Fig. S4B). Furthermore, expression of the genomic fragment of *AtABCG34* (*ABCG34pro:sGFP:ABCG34;* gDNA) rescued the mutants from sensitivity to *A. brassicicola* (Fig. 2 A-C).

***AtABCG34* expression is induced by methyl jasmonate and necrotrophic pathogens**

We then analyzed whether the expression level of *AtABCG34* changes in response to treatment with either methyl jasmonate (MeJA) or salicylic acid (SA), hormones that are known to function in the pathogen defense response. *AtABCG34* expression was induced up to 7-fold within 1 h of MeJA treatment (Fig. 3A) but was only slightly induced by SA treatment (Fig. 3B). Next, we analyzed the transcript levels of *AtABCG34* in plants exposed to necrotrophic fungi (*A. brassicicola* and *B. cinerea). AtABCG34* transcript levels increased 3- to 6-folds in a time-dependent manner in response to necrotrophic fungal pathogen treatments (Fig. 3C and Fig. S5A).

GUS staining of *ABCG34pro:GUS* lines at 3 days post inoculation (dpi) also revealed the high expression of *AtABCG34* around the *B. cinerea* infection sites (Fig. S5B). Thus, *AtABCG34* expression was strongly induced by necrotrophic fungal pathogens (*A. brassicicola* and *B. cinerea*) and MeJA, but not by SA.

AtABCG34 displays polar localization at the outer surface of plasma membrane of

epidermal cells

Next, we examined the sub-cellular localization of AtABCG34 in complementation lines expressing *ABCG34$_{pro}$:sGFP:ABCG34* in the *atabcg34-1* background. The leaves of the transgenic plants were stained with FM4-64 for only 10 min on ice to prevent the dye from entering the cells. Under this condition, the red fluorescence of FM4-64 delineated only the plasma membrane, and the green fluorescence of sGFP-ABCG34 was co-localized with the red fluorescence (Fig. 3D), suggesting that AtABCG34 is localized to the plasma membrane. Interestingly, observation of the transverse sections of the leaves revealed that AtABCG34 was polarly localized at the outer half of the epidermal cells both at the adaxial and abaxial surfaces (Fig. 3E). A similar pattern of polar localization at the outer surface of the epidermal cells was observed in the root (Fig. 3F).

To determine whether pathogens affect AtABCG34 localization, we observed sGFP fluorescence in leaves expressing *ABCG34$_{pro}$:sGFP:ABCG34* in the *atabcg34-1* background. When treated with *A. brassicicola,* green fluorescence of sGFP:ABCG34 increased continuously until 24 hours post inoculation (hpi; Fig. 3 G and H), indicating induction of AtABCG34 by the pathogen, in agreement with the results of our qRT-PCR analysis (Fig. 3C and Fig. S5A) and GUS expression assay (Fig. S5B). Interestingly, in contrast to non-treated plants (Mock), the fluorescence was localized not only at the plasma membrane, but also in dot-like structures in the cells (Fig. 3G).

***atabcg34* exhibits reduced camalexin abundance at the leaf surface**

The polar localization of AtABCG34 at the plasma membrane and hypersensitivity of *atabcg34* to necrotrophic pathogens suggest that AtABCG34 may be required for the secretion of chemicals that protect plants from pathogen attack. Two different classes of

192 such chemicals may be involved in this process: surface coating materials, as shown for
193 AtABCG32/PEC1 (21, 22), and secondary metabolites, as shown for
194 AtABCG36/PDR8/PEN3 (14). The first possibility was tested by an ethanol penetration
195 assay which detects permeability defect. However, we could not observe any difference in
196 ethanol penetration between the wild type and *atabcg34* mutants (Fig. S6A).

197 To test the second possibility (i.e. AtABCG34 mediates the secretion of secondary
198 metabolites), we compared the levels of some secondary metabolites between the wild type
199 and the *atabcg34* mutants. The levels and the kinds of phenolic compounds in plants
200 infected with *B. cinerea* did not differ between the *atabcg34* mutants and wild type (Fig.
201 S6B). Furthermore, there was no distinct difference in glucosinolate content in plants
202 infected by *A. brassicicola* (Fig. S6C). Camalexin is a major phytoalexin produced by *A.*
203 *thaliana* and other Brassicaceae and is known to be induced by *A. brassicicola* infection,
204 and to be required for resistance against *A. brassicicola* (23). Consequently, we determined
205 the camalexin contents at the surface of whole rosettes and observed that it was reduced to
206 about half in *atabcg34* mutants compared to the wild type both at 24 hpi (Fig. 4A) and 48
207 hpi with *A. brassicicola* (Fig. S6D). The complementation lines had similar levels of
208 rosette leaf surface camalexin as the wild type at 24 hpi (Fig. 4A). Total camalexin content
209 of the whole rosette of *atabcg34* mutants was also reduced compared to that of the wild
210 type at 24 and 48 hpi with *A. brassicicola* (Fig. 4B). These data suggest that AtABCG34 is
211 necessary for camalexin secretion to the surface upon *A. brassicicola* infection.

212 We further tested this possibility by generating *AtABCG34* overexpression lines in
213 the wild-type background. The rosette leaves of plants expressing $35S_{pro}$*:sGFP:ABCG34*
214 (OE1-OE3) exhibited higher levels of surface camalexin at 24 hpi than did the wild type
215 rosette leaves (Fig. 4A). The increased secretion of camalexin was accompanied by

improved disease resistance to *A. brassicicola* (Fig. 4C-E); the lesion diameter and pathogen growth were significantly reduced in all three overexpression lines treated with this pathogen compared to the wild type (Fig. 4 D and E).

AtABCG34 expression improves tolerance to camalexin in *A. thaliana* and BY2 cells

As camalexin is known to be toxic to *A. thaliana* suspension culture cells (24), we next compared the effect of exogenously applied camalexin on the mature leaf surface of wild-type and *atabcg34* mutants. Cell death induced by camalexin treatment was analyzed by Evans blue staining. The leaves of both *atabcg34* mutants exhibited significantly higher rates of cell death than did the wild type and complementation lines in response to camalexin treatment. However, the cell death response in the leaves of the *atpad3-1* mutant, which has a point mutation in the gene encoding a key enzyme in camalexin biosynthesis and exhibits susceptibility to *A. brassicicola* (25), did not differ in cell death from that of the wild type or the complementation lines following camalexin treatment (Fig. 5A, middle panel). By contrast, *atabcg34* and *atpad3-1* mutants were similar in their responses to *A. brassicicola* treatment, exhibiting significantly increased levels of cell death compared to the wild type and complementation lines (Fig. 5A, bottom panel).

We then tested whether AtABCG34 can confer camalexin tolerance in a heterologous system. For this purpose, we expressed *$35S_{pro}$:sGFP:ABCG34* (cDNA) in tobacco Bright Yellow 2 (BY2) cells. AtABCG34 was localized at the plasma membrane in BY2 cells (Fig. 5B, middle and bottom panels), similarly as in *A. thaliana* cells (Fig. 3D), by contrast to the cytosolic localization of free sGFP (EV, Fig. 5B, top panel). When cultured in medium containing camalexin, AtABCG34-expressing BY2 cells (ABCG34-1 and ABCG34-2) exhibited reduced rates of cell death (Fig. 5C) and increased cell density

(Fig. 5D) compared to the EV expressing cells.

AtABCG34 contributes to pre-invasion resistance against *A. brassicicola*

Plants exhibit a multi-layered defense response to *A. brassicicola* that is composed of pre- and post-invasion stages. Formation of an appressorium, a swollen structure at the tip of growing hyphae that penetrates the plant cell wall (26), marks the pre-invasion stage. Under our experimental conditions, appressoria were observed at 18 hpi with *A. brassicicola* (Fig. 3G), consistent with a previous report that appressoria formed at 12–24 hpi with *A. brassicicola* (27). Since *AtABCG34* expression induced by *A. brassicicola* treatment was apparent at 12 hpi (Fig. 3 C and H), a relatively early time point during the pathogen defense response (i.e., before appressorium formation), we suspected that AtABCG34 might contribute to resistance at the pre-invasion stage. We tested this possibility using three different methods. First, we counted the pathogen penetration sites by callose staining in the wild type, *atabcg34* mutants, and complementation lines. Callose is deposited at the penetration site in response to *A. brassicicola* treatment (28), and a high number of callose depositions indicate a failure to overcome the pathogen at the pre-invasion stage (5, 29). *atabcg34* mutants exhibited a significantly higher number of penetration sites than did the wild type and complementation lines (Fig 6 A and B). We also analyzed the *atpad3-1* mutant and found that it exhibited a high penetration frequency, similarly to the *atabcg34* mutants (Fig. 6 A and B). These results support the notion that the reduction of camalexin content/secretion compromised defense against *A. brassicicola* at the pre-invasion stage. Second, we examined the *A. brassicicola* conidia germination in the wild type and AtABCG34 over-expressing lines. We found that overexpression lines exhibited significantly lower rates of conidia germination than did

the wild type (Fig. 6C), which indicates that the AtABCG34 plays an important role in preventing the conidia germination before invasion to the leaf. Third, we tested whether *PDF1.2* induction by pathogens differs between the wild type and the mutants. *PDF1.2* is induced by *A. brassicicola* infection and plays an important role in the pre-invasion stage of resistance (30). When inoculated with *A. brassicicola* or *B. cinerea, PDF1.2* expression increased in both wild-type and the mutants, but the extent of the increase was significantly less in *atabcg34* mutants than in the wild type (Fig. 6D).

Accessions assay to evaluate the contribution of AtABCG34 to resistance against *A. brassicicola*

Next, we asked whether AtABCG34 is an important factor in determining the defense response to *A. brassicicola* among natural *Arabidopsis* accessions. To address this question, we used *Arabidopsis* accessions that were reported to exhibit different levels of resistance to *A. brassicicola* infection (31): Dijon-G and C24 with susceptible phenotypes; Aua/Rhon (Aa), Cape Verde (Cvi), RLD-1 and Columbia-0 (Col-0) with intermediate resistance; and Kendallville, Muehlen (Mh), Ksk-1, Turk Lake (Tul-0), Bensheim (Be-0) and Nossen (No-0) with resistant phenotypes. We evaluated the different accessions for their *AtABCG34* transcript levels and their sensitivity to *A. brassicicola* inoculation. The responses of the accessions to *A. brassicicola* fell into two categories. Consistent with the results of a previous report (31), the susceptible group included Dijon-G, C24, Aua, RLD-1, Col-0, and Cvi (Fig. 7 A and B). Contrary to the results of the previous report (31), accessions No-0 and Be-0 were also susceptible to *A. brassicicola* under our experimental conditions (Fig. 7 A and B).The more resistant group included the remaining accessions.

Four out of the 7 susceptible accessions, No-0, Aua, RLD-1, and Be-0, expressed

AtABCG34 at similar or lower levels than did Col-0 (Fig. 7C). The three remaining susceptible accessions, Dijon-G, C24, and Cvi, expressed *AtABCG34* at 5- to 6-fold higher levels than did Col-0. By contrast, three of the four more resistant accessions, Kendallville, Ksk-1, and Mh, expressed *AtABCG34* at 4- to 41-fold higher levels than did Col-0. The *AtABCG34* overexpression lines we generated fell into the more resistant group and expressed *AtABCG34* at 14- to 33-fold higher levels than did Col-0. Among the more resistant accessions, Tul-0 was the only accession that expressed *AtABCG34* at a level comparable to Col-0.

To quantify the relationship between *AtABCG34* expression level and pathogen growth in different accessions and overexpression lines, we performed regression analysis. The coefficient of correlation was -0.27 when only the 12 accessions were included in the analysis (Fig. 7D), indicating a weak negative correlation between pathogen growth and *AtABCG34* expression levels in the accessions tested. However, the coefficient of correlation changed to -0.54 when three overexpression lines were included together with the 12 accessions (Fig. 7E), indicating a moderate negative correlation between pathogen growth and expression levels of *AtABCG34*.

Discussion

AtABCG34 is important for defense against necrotrophic fungi

In this study, we identified AtABCG34 as a strong factor conferring tolerance to the antifungal diterpene sclareol (Fig. 1 and Fig. S2), and hence as a potential player in pathogen defense. We report three lines of evidence supporting the role of AtABCG34 in defense against necrotrophic fungal pathogens. First, *atabcg34* mutants exhibited

hypersensitivity to the necrotrophic fungi, *A. brassicicola* (Fig. 2) and *B. cinerea* (Fig. S4A). Second, *AtABCG34* expression was induced by *A. brassicicola* (Fig. 3C, G and H) and *B. cinerea* (Fig. S5) infection in a time-dependent manner. Third, *AtABCG34* expression was induced substantially by the application of MeJA (Fig. 3A), and only slightly by SA (Fig. 3B). The induction of *AtABCG34* by MeJA and necrotrophic fungal pathogens is similar to that observed for the NpPDR1 and NtPDR1 transporters, which secrete antifungal molecules in response to pathogen infection (32). MeJA was reported to be important for necrotrophic pathogens rather than biotrophic pathogen resistance (33). Moreover, JA, but not SA, is necessary for the resistance to *A. brassicicola,* as evidenced by the reduced tolerance of a JA signaling mutant, *coi1,* to the pathogen, and the similar tolerance levels of SA signaling mutant, *npr1* and SA deficient, *NahG* expressing plants, to the pathogen compared to the wild type, respectively (33). The pattern of *AtABCG34* induction (Fig. 3) suggests that AtABCG34 is involved in the defense against *A. brassicicola* through the JA signaling pathway but not through the SA signaling pathway. AtABCG34 does not seem to be involved in biotrophic pathogen resistance since, i) it was not induced much by SA, which is of major importance for biotrophic pathogen resistance (34), and ii) the *atabcg34* mutants did not exhibit sensitivity to the biotrophic bacterial pathogen *Pst* DC3000 (Fig. S4B).

Possible importance of AtABCG34 in natural habitat

In nature, multiple factors usually contribute to a phenotype. Thus, in an accession study, a very high correlation between the level of one factor and the phenotype is rare (35, 36). Consistently, in our results as well, there was only a weak negative correlation between *A. brassicicola* growth and *AtABCG34* expression levels

(Fig. 7D). However, there was a significant, moderate negative correlation when overexpression lines were included together with the 12 accessions in the statistical analysis (Fig. 7E). Moreover, three out of the four ecotypes resistant to *A. brassicicola* expressed *AtABCG34* at higher levels than did Col-0, whereas only three out of the seven susceptible accessions did so (Fig. 7C). These results suggest that AtABCG34 contributes to the disease resistance in naturally occurring genetic variants. AtABCG34 may be one among many different factors contributing to *A. brassicicola* resistance, and only a subset of the accessions may have evolved this strategy. Other factors contributing to *A. brassicicola* resistance include other JA-response pathways (37), other secondary metabolites (such as phenolics), and a mechanism to tolerate the toxins secreted by the pathogen (31). Further studies, including analyses of additional accessions for fungal disease resistance, are necessary to evaluate this hypothesis.

It is interesting that the expression level of *AtABCG34* in the Kendallville accession was about 41 times higher than that in Col-0. Thus, in wild populations of *Arabidopsis*, there may be a wide range of expression levels of this gene. However, we do not expect that there would be many other accessions with even higher levels of expression of *AtABCG34* than the Kendallville ecotype, because OE1 and OE3 lines expressed *AtABCG34* at the levels lower than that found in this accession, but exhibited similar levels of resistance to *A. brassicicola* (Fig. 7B).

AtABCG34 localization before and after *A. brassicicola* infection

AtABCG34 was localized at the outward-facing sides of the plasma membrane in epidermal cells of the leaves and roots (Fig. 3 E and F). Such polar localization of ABC transporters was reported previously for AtABCG32 (21), AtABCG36 and AtABCG37

(38). These transporters secrete compounds important for cuticle formation (21) or defense (13), or transport auxin precursor to the rhizosphere (39), respectively. The polar localization of AtABCG34 suggests that it secretes some compounds to the leaf surface. The mechanism of polar localization of AtABCG34 might resemble that of AtABCG36, another ABCG sub-family member involved in pathogen defense; i.e., polar secretion, constitutive endocytic recycling, and restricted lateral diffusion (40).

AtABCG34 is highly induced by *A. brassicicola* infection (Fig. 3 C and H), and accumulates at the plasma membrane, as indicated by the increase in sGFP:ABCG34 fluorescence when plants are infected with the pathogen (Fig. 3G). Previous studies of AtABCG36/PEN3 and NbABCG1/2 showed that these transporters are preferentially localized at the pathogen penetration sites (5, 11). However, we did not observe such preferential accumulation of AtABCG34 at the penetration site. Rather, we observed its accumulation at broad areas surrounding the inoculation site of *A. brassicicola* (Fig. 3G) and *B. cinerea* (Fig. S5B). Interestingly, *A. brassicicola* infection also induced accumulation of sGFP:ABCG34 in dot-like structures that, to our knowledge, have not been reported for plant transporters during pathogen infection. Further studies are needed to decipher the formation and function of these dot-like structures.

AtABCG34 most likely transports camalexin

Our data described above indicate that AtABCG34 is involved in transporting secondary metabolites to the leaf surface to inhibit growth of necrotrophic pathogens. Initially, we selected AtABCG34 based on a screen for hypersensitivity to sclareol, a diterpene alcohol. However, based on several independent lines of evidence, we propose that the secondary metabolites that AtABCG34 transports include an indole alkaloid,

384 camalexin (Fig. 8). First, surface camalexin in the rosette leaves was significantly reduced
385 in *atabcg34* mutants (Fig. 4A and Fig. S6D), whereas the surface camalexin levels were
386 increased in the AtABCG34-overexpressing lines (Fig. 4A). Second, expression of
387 sGFP:ABCG34 in BY2 cells improved resistance to a toxic concentration of camalexin
388 (Fig. 5B-D), which suggests that AtABCG34 mediates removal of camalexin from the BY2
389 cells. Third, when treated with exogenous camalexin, *atabcg34* mutants exhibited high
390 levels of cell death, but the *atpad3-1* mutant did not (Fig. 5A). This is most likely because
391 the functional AtABCG34 in the *atpad3-1* mutant plant cells was able to secrete camalexin
392 from the cells. By contrast, there was no difference in the cell death responses of *atpad3-1*
393 and *atabcg34* mutants to *A. brassicicola* treatment, indicating that both camalexin
394 synthesis and transport are necessary to resist against *A. brassicicola* infection. Fourth, the
395 *atpad3-1* mutant exhibited similar *A. brassicicola* penetration frequency as the *atabcg34*
396 mutants (Fig. 6 A and B). This result is consistent with our explanation that the two
397 proteins function in the same pathway of defense against the pathogen: whereas PAD3
398 catalyzes the biosynthesis of camalexin, AtABCG34 mediates transport of camalexin. Fifth,
399 both AtABCG34 (Fig. 3G and Fig. S5B) and the camalexin biosynthesis genes (41) are
400 induced around the *A. brassicicola* and *B. cinerea* infection site. By contrast, we did not
401 obtain any clear evidence that the transporter transports surface coating material (Fig. S6A).
402 Neither was there any clear difference in the levels of phenolics (in plants infected by *B.*
403 *cinerea)* nor glucosinolates (in plants infected by *A. brassicicola*) between the *atabcg34*
404 and wild-type plants (Fig. S6 B and C). AtABCG34 might transport multiple substrates,
405 such as an indole alkaloid camalexin and some diterpene alcohols similar to sclareol
406 produced by *A. thaliana*. This would not be unusual, since a single ABCG transporter can
407 transport many chemically unrelated substrates (42, 43), and ABCG transporters have a

broad range of substrates, including alkaloids, terpenoids, various hormones, and lipids (42).

In addition, a comparison of our results with some previous reports support that AtABCG34 is involved in camalexin transport. Similar to AtABCG34, camalexin biosynthesis is induced by necrotrophic fungal pathogens (44). AtABCG34 is induced in response to JA (Fig. 3A) and JA signaling components are involved in the biosynthesis of camalexin (25). Interestingly, a full-size ABCG transporter, BcatrB, in *B. cinerea* is necessary for the export of camalexin (45). This transporter is a critical virulence factor, as evidenced by the failure of a *BcatrB* knockout mutant to infect *A. thaliana*. Thus, there may have been an evolutionary arms race between plants and the pathogen to develop camalexin transporters; plants developed ABC transporters to secrete camalexin, and fungal pathogens developed similar ABC transporters to export camalexin from their cytosol. Evolutionary studies on these transporters may lead to interesting findings on co-evolution.

We attempted to conduct camalexin transport assays using BY2 cells. However, we did not find any conditions that allowed time-dependent loading of camalexin into cells. Similar difficulties in carrying out transport assays were reported for sclareol in BY2 cells (2). Direct transport assays of these secondary metabolites await further understanding of the chemical nature and permeability of the chemicals through lipid membranes. Nonetheless, our results strongly suggest that AtABCG34 has a critical role in secreting camalexin to the surface of the plant, where it inhibits invasion of *A. brassicicola*.

Since the level of surface camalexin was reduced to half that of the wild type, we propose that other mechanisms, such as diffusion, or other transporters, such as ABC transporters, mediate the secretion of the remaining half of camalexin to the leaf surface.

The only other ABCG member that has been reported to affect camalexin levels is AtABCG36; an increase in total camalexin content was observed in the *pdr8/pen3/abcg36* mutant in response to powdery mildew fungal infection (46). However, it is unclear whether the *pdr8* mutant has increased levels of surface camalexin and this mutant has not been tested for its response to *A. brassicicola* or *B. cinerea*. Thus, it remains to be determined whether there are additional ABCG transporters for camalexin.

AtABCG34 functions at the pre-invasion stage

Some accessions of *Arabidopsis* exhibit an incompatible interaction with *A. brassicicola* and have evolved two layers of defense: pre- and post-invasion defense (47). Pre-invasion defense culminates when the pathogen tries to penetrate the plant cell. Four of our findings suggest that AtABCG34 functions at the pre-invasion step of defense. First, the level of camalexin was reduced in *atabcg34* mutants compared to the wild type (Fig. 4 A and B, Fig. S6D). Camalexin, a major phytoalexin in *A. thaliana* is known to be important for pre-invasion resistance against powdery mildew, and *atpad3-1*, a camalexin deficient mutant, is defective in the pre-invasion resistance to both powdery mildew (48) and *A. brassicicola* (33). Second, *A. brassicicola* conidia germination was significantly reduced in the AtABCG34 overexpression lines (Fig. 6C), which had higher levels of surface camalexin (Fig. 4A). Inhibition of conidia germination on the plant surface is most likely due to the higher level of camalexin secreted by AtABCG34. Third, *atabcg34* mutants exhibited higher penetration frequency than did the wild type, and wild-type levels of penetration were restored in the complementation lines (Fig. 6A and B). Furthermore, the *atpad3-1* mutant also exhibited high penetration frequency similar to the *atabcg34* mutants. In general, mutants compromised in pre-invasion defense exhibit high penetration frequency

(marked by callose deposition) at the inoculation site (29, 49). Fourth, the expression levels of *AtPDF1.2,* a JA and *A. brassicicola* responsive-gene, were significantly reduced in *atabcg34* mutants compared to the wild type (Fig. 6D). *AtPDF1.2* is induced in response to necrotrophic fungal pathogens and JA (50), similar to *AtABCG34*, and constitutive expression of *PDF1.2* enhances pre-invasion resistance (30). These results indicate that AtABCG34 has an important function in pre-invasion resistance.

Other ABC transporters important for resistance at the pre-invasion stage include NtPDR1 and NpPDR1, which transport sclareol (2, 3), an important factor for pre-invasion resistance (5). Recently, NbABCG1 and NbABCG2 were reported to be important for both pre- and post-invasion resistance in *N. benthamiana* (5).

Application potentials of AtABCG34

Our data revealed that AtABCG34 is an important factor required for defense against necrotrophic fungal pathogens, *A. brassicicola* and *B. cinerea*, that functions by secreting camalexin to the surface. *A. brassicicola* infection results in dark leaf spots on most *Brassica* species, including economically-important oilseed crops (51). Infection by *A. brassicicola* considerably reduces the quality and quantity of harvested *Brassica* crops (52); resulting in annual yield losses of 15 to 70% (52). Interestingly, overexpression of AtABCG34 enhanced the surface camalexin content in *A. thaliana* (Fig. 4A) and resistance to *A. brassicicola* (Fig. 4C). We predict that high levels of *AtABCG34* expression in economically important *Brassica* species, such as *B. napus* and *B. oleracea,* will be associated with reduced disease severity and yield loss following *A. brassicicola* infection due to increased secretion of camalexin to the plant's surface. Such a goal may be attained by genetic approaches or by screening and selecting for accessions of *B. napus* and *B.*

oleracea that have naturally high levels of expression of the *ABCG34* orthologue.

Materials and Methods

Plant Materials and Growth Conditions

A. thaliana (L.) Heynh. ecotype Col-0 wild-type (WT) and transgenic plants were grown on half-strength Murashige-Skoog (½MS) agar plates with 1% sucrose in the presence or absence of sclareol (65 µM) and grown for 2-3 weeks at 16/8 h light/dark, 22/18°C cycle). For long-term experiments, plants were transferred to soil and grown in a controlled growth chamber (16/8 h light/dark; 22/18°C). For pathogen infection and camalexin analysis, 3- to 4-week-old plants were used. For accessions analysis: Kendallville (CS76344), Bensheim (Be-0- CS76345), Aua/Rh¨on (CS900), Cape Verde (Cvi-CS902), Muehlen (Mh-CS904), C24 (CS906), Dijon-G (CS910), Col-0 (CS1092), Ksk-1 (CS1634), Rld-1 (CS76588), Tul-0 (CS76618), No-0 (CS28564) were used.

Fungal Culture and Disease Assays

Botrytis cinerea was grown on 2 X V8 agar (36% V8 juice, 0.2% $CaCO_3$, and 2% Bacto-agar) at 25°C for 1- to 2-weeks and spores were resuspended in 1% Sabouraud maltose broth buffer (SMBB, Difco). *A. brassicicola* strain KACC40036 was grown on potato dextrose agar and resuspended in distilled water for plant inoculation (53). To examine gene expression patterns, whole *A. thaliana* plants were inoculated with *B. cinerea* or *A. brassicicola* by spraying with a spore suspension (5 X 10^5 spores/ml) in SMBB or distilled water, respectively. For the disease assay, 8 µl of spore suspension (5 X 10^5 spores/ml) was dropped onto detached leaves. Inoculated leaves were kept under high humidity until 5 dpi. *B. cinerea* spore population was counted as described previously

(23). *A. brassicicola* growth was quantified as follows: leaf discs were collected at 5 dpi from the infection area, using a No. 2 cork borer. The gDNA was extracted and quantitative PCR was performed as described previously (54). To estimate the growth of *A. brassicicola,* Cutinase A (*ABU03393)* DNA was amplified using primers listed in Table S1. The value was normalized by amplifying genomic DNA of *A. thaliana α-Shaggy kinase* (*At5g26751*), using iASK1 and iASK2 primers (Table S1). Standard curves were prepared using gDNA extracted from the *A. thaliana* leaf discs and *A. brassicicola* grown on potato dextrose agar plates. For the intact-plant assay, 10 µl of spore suspension (5 X 10^5 spores/ml) in distilled water was dropped on the fully-expanded leaves of 4-week-old plants.

Camalexin Level Assay

Four-week-old plants were sprayed with spore suspension (5 X 10^5 spores/mL) of *A. brassicicola* and whole rosettes were collected at indicated time points. Total camalexin was extracted with hot methanol and chloroform, and surface camalexin was extracted with dichloromethane, using established protocols (55, 56) with slight modifications. To extract surface camalexin, rosette leaves of *A. thaliana* were gently rotated in dichloromethane for 30 s. Extracted samples were loaded onto TLC plate and separated, and camalexin band was visualized by its blue fluorescence under an ultraviolet lamp (365 nm). The silica containing camalexin was scraped off the plate and camalexin was extracted into 500 µl of methanol. The emission at 385 nm after excitation at 315 nm was measured to quantify the camalexin in 96-well black microplate (Greiners, Frickenhausen, Germany) with Tecan fluorometer (M200PRO). The camalexin concentration was calculated by comparison with a standard curve obtained using

commercially available camalexin purchased from Glixx Lab (Southborough, MA).

Camalexin Toxicity Assay

Three-week-old plants were treated with 1% DMSO (solvent control treatment), 1 mg/ml camalexin, or 5 X 10^5 spores/ml of *A. brassicicola* (positive control). Evans blue staining was performed 24 h after treatment as described previously (57). Briefly, 0.1% Evans blue solution (w/v) was vacuum infiltrated (25 mm of Hg for 5 min, followed by a 5-min hold and subsequent slow release) and the leaves were stained for 8 h at room temperature. After staining, samples were washed with a phosphate-buffered saline solution containing 0.05% (v/v) Tween-20 until the washing solution became clear.

For BY2 cells, the 6-day-old culture was treated with 250 μM camalexin for 30 min at 25°C in darkness (24). The cells were washed with water, harvested by centrifugation (at 13,800 g for 5 min at room temperature). To analyze cell death, cells were stained with 0.05% Evans blue for 15 min at 25°C, and then washed three times with water (57). Evans blue stain was extracted from the cells with 50% methanol+1% SDS for 60 min at 60°C and blue color was quantified by measuring absorbance at 595 nm and normalized by optical density at 600 nm (O.D.). Cell death caused by boiling, used as a positive control, was set to 100% and relative cell death caused by either DMSO or camalexin treatment was analyzed. For cell growth analysis, a 3-day-old culture was treated with either 0.01% DMSO (solvent control) or camalexin (50 μM), and O.D. at 600 nm was measured 3 days after camalexin treatment using a spectrophotometer.

Callose Staining

552 Callose staining was performed as described previously (12). Briefly, 3- to 4-week-old
553 plants were treated with *A. brassicicola* (5 X 10^5 spores/ml) solution. Leaf discs from the
554 inoculation sites were collected 24 hpi and fixed in ethanol: acetic acid (3:1) by brief
555 vacuum infiltration (at 25 mm of Hg for 5 min, followed by a 5-min hold and subsequent
556 slow release) and de-stained by gentle rotation until the disks became translucent,
557 washed with 150 mM K_2HPO_4 for 30 min, and stained with aniline blue (1%) staining
558 solution for 2 h on a shaker. Stained discs were observed with a Zeiss fluorescence
559 microscope (Axioskop 2 MOT) using the DAPI channel after mounting with 50%
560 glycerol.
561
562 **Regression analysis between *AtABCG34* expression and pathogen growth in natural**
563 **accessions**
564 The expression levels of *AtABCG34* and pathogen growth in different ecotypes were
565 analyzed as mentioned above using sets of primers listed in Table S1. The *AtABCG34*
566 sequences of all ecotypes tested contained fragments that precisely matched the sequences
567 of the primers used. However, the Tubulin 8 sequences differed from those of the primers
568 (both forward and reverse) at one base pair in two ecotypes: Kendallville and RLD-1.
569 However, the transcript levels of Tubulin 8 in these two ecotypes were similar to those of
570 other the ecotypes evaluated.
571 The Ksk-1 and Bensheim ecotypes have not been sequenced. Thus, we sequenced
572 parts of the coding regions of *AtTubulin 8* and *AtABCG34*. No differences were observed in
573 the regions corresponding to the *AtABCG34* primer sequences in either of the two ecotypes.
574 One base pair change was detected in the center of both the forward and reverse primers of
575 *AtTubulin 8* in Bensheim. The Tubulin 8 sequence of Ksk-1 differed at 3 base pairs of the

forward primer. Thus, a new forward primer (listed in Table S1) was designed to compare the transcript levels of Tubulin 8 in Ksk-1 and Col-0.

Regression analysis between *AtABCG34* expression and pathogen growth was performed by comparing the Pearson's correlation coefficient between average data of *AtABCG34* expression and pathogen growth with 10,000 randomly permuted data sets from all 12 accessions either including or excluding 3 overexpression (OE1-OE3) lines. Logarithmic values of relative copy numbers of the *Cutinase A* of *A. brassicicola* were used for pathogen growth.

For other methods check SI Materials and Methods

Footnotes

[1]K.-H.P. and Y.L. contributed equally to this work.

[2]To whom the correspondence may be addressed. Email: ylee@postech.ac.kr.

Author contributions: D.K., H.C., S.H., K-H.P. E.M., K.H.S., and Y.L. designed the research. D.K., H.C., and S.H. performed the experiments. B.B. measured the phenolics. J.K. participated in accession analysis. D.K., E.M., K.H.S., K.-H.P., and Y.L. wrote the article.

Conflict of interest statement: Authors declare no conflict of interest.

Acknowledgments

This work was supported by a National Research Foundation (NRF) of Korea grant funded by the Ministry of Science, Information and Communication Technology, and Future Planning, Korea awarded to Y.L. (NRF-2015R1A2A1A01004294), and a grant awarded to K.-H.P. from the NRF funded by the Korean government (MSIP) (No.

R1A2A2A01002476). We thank Professor Jane Glazebrook for kindly providing us with camalexin and Dr. C. Douglas Grubb for measuring glucosinolates.

References:

1. Srikantaramas S, Yamazaki M, Saito K (2008) Mechanisms of resistance to self-produced toxic secondary metabolites in plants. *Phytochem Rev* 7: 467–477.
2. Crouzet J, Roland J, Peeters E, Trombik T, Ducos E, Nader J (2013) NtPDR1, a plasma membrane ABC transporter from *Nicotiana tabacum*, is involved in diterpene transport. *Plant Mol Biol* 82: 181–192.
3. Jasinski M, Stukkens Y, Degand H, Purnelle B, Marchand-Brynaert J, Boutry, M (2001) A plant plasma membrane ATP binding cassette-type transporter is involved in antifungal terpenoid secretion. *The Plant Cell* 13: 1095–1107.
4. Stukkens Y, Bultreys A, Grec S, Trombik T, Vanham D, Boutry M (2005) NpPDR1, a pleiotropic drug resistance-type ATP-binding cassette transporter from *Nicotiana plumbaginifolia*, play a major role in plant pathogen defense. *Plant Physiology* 139: 341–352.
5. Shibata Y, Ojika M, Sugiyama A, Yazaki K, Jones DA, Kawakita K, Takemoto D (2016) The Full-size ABCG transporters Nb-ABCG1 and Nb-ABCG2 function in pre- and post-invasion defense against *Phytophthora infestans* in *Nicotiana benthamiana*. *The Plant Cell* 28: 1163-1181.
6. Bienert MD, Siegmund SEG, Drozak A, Trombik T, Bultreys A, Baldwin IT, Boutry M (2012) A pleiotropic drug resistance transporter in *Nicotiana tabacum* is involved in defense against the herbivore *Manduca sexta*. *The Plant Journal* 72: 745-757.

624 7. Sasse J, Schlegel M, Borghi L, Ullrich F, Lee M, Liu G-W, Giner J-
625 L, Kayser O, Bigler L, Martinoia E (2016) *Petunia hybrida* PDR2 is involved in
626 herbivore defense by controlling steroidal contents in trichomes. *Plant Cell & En*
627 *vironment* 39: 2725-2739.
628 8. Yu F, Luca VD (2013) ATP-binding cassette transporter controls leaf surface
629 secretion of anticancer drug components in *Catharanthus roseus*. *Proc. Natl. Acad.*
630 *Sci USA* 110: 15830–15835.
631 9. Krattinger SG, Lagudah ES, Spielmeyer W, Singh RP, Huerta-Espino J, McFadden
632 H, Bossolini E, Selter LL, Keller B (2009) A putative ABC transporter confers
633 durable resistance to multiple fungal pathogens in wheat. *Science* 323: 1360-1363.
634 10. Krattinger SG, Sucher J, Selter LL, Chauhan H, Zhou B, Tang M, Upadhyaya MN,
635 Mieulet D, Guiderdoni E, Weidenbach D, Schaffrath U, Lagudah ES, Keller B
636 (2016) The wheat durable, multipathogen resistance gene Lr34 confers partial
637 blast resistance in rice. *Plant Biotechnology Journal* 14: 1261–1268.
638 11. Underwood W, Somerville SC (2013) Perception of conserved pathogen
639 elicitors at the plasma membrane leads to relocalization of the *Arabidopsis*
640 PEN3 transporter. *Proc. Natl. Acad. Sci. USA* 110: 12492-12497.
641 12. Clay NK, Adio AM, Denoux C, Jander G, Ausubel FM (2009) Glucosinolate
642 metabolites required for an *Arabidopsis* innate immune response. *Science* 323:
643 95–101.
644 13. Stein M, Dittgen J, Sánchez-Rodriguez C, Hou B-H, Molina A, Schulze-Lefert P,
645 Lipka V, Somerville S (2006) *Arabidopsis* PEN3/PDR8, an ATP binding cassette
646 transporter, contributes to nonhost resistance to inappropriate pathogens that enter
647 plants by direct penetration. *The Plant Cell* 18: 731–746.

14. Lu X, Dittgen J, Piślewska-Bednarek M, Antonio MA, Schneider B, Doubský AS J, Schneeberger K, Weigel D, Bednarek P, Schulze-Lefert P (2015) Mutant allele-specific uncoupling of PEN3 functions reveals engagement of the ABC25 transporter in distinct tryptophan metabolic pathways. *Plant Physiology* 168: 814–827.
15. Campbell EJ, Schenk PM, Kazan K, Penninckx IA, Anderson JP, Maclean D J, Cammue BP, Ebert P R, Manners JM (2003) Pathogen-responsive expression of a putative ATP-binding cassette transporter gene conferring resistance to the diterpenoid sclareol is regulated by multiple defense signaling pathways in *Arabidopsis*. *Plant Physiology* 133: 1272– 1284.
16. Kang J, Park J, Choi H, Burla B, Kretzschmar T, Lee Y, Martinoia E (2011) Plant ABC transporters. *The Arabidopsis book/American Society of Plant Biologists* 9: p. e0153.
17. Ji H, Peng Y, Meckes N, Allen S, Stewart JCN, Traw MB (2014) ATP-dependent binding cassette transporter G family member 16 increases plant tolerance to abscisic acid and assists in basal resistance against *Pseudomonas syringae Pst* DC3000. *Plant Physiology* 166: 879–888.
18. Yazaki K. (2006) ABC transporters involved in the transport of plant secondary metabolites. *FEBS letters* 580: 1183-1191.
19. Bailey JA, Garter GA, Burden RS, Wain RL (1975) Control of rust diseases by diterpenes from *Nicotiana glutinosa. Nature* 255: 328-329.
20. Kennedy BS, Nielsen MT, Severson RF, Sisson VA, Stephenson MK, Jackson DM (1992) Leaf surface chemicals from *Nicotiana* affecting germination of *Peronospora tabacina* (Adam) sporangia. *Journal of Chemical Ecology* 18: 1467-

672 1479.
673 21. Bessire M, Borel S, Fabre G, Carrac L, Efremova N, Yephremov A, Cao Y, Jetter
674 R, Jacquat A-C, Metraux J, Nawratha C (2011) A member of the PLEIOTROPIC
675 DRUG RESISTANCE family of ATP binding cassette transporters is required for
676 the formation of a functional cuticle in *Arabidopsis*. *The Plant Cell* 23: 1958-1970.
677 22. Fabre G, Garroum I, Mazurek S, Daraspe J, Mucciolo A, Sankar M, Humbel BM,
678 Nawrath C (2016) The ABCG transporter PEC1/ABCG32 is required for the
679 formation of the developing leaf cuticle in *Arabidopsis*. *New Phytologist* 209:
680 192–201.
681 23. Wees SCV, Chang HS, Zhu T, Glazebrook J (2003) Characterization of the early
682 response of *Arabidopsis* to *Alternaria brassicicola* infection using expression
683 profiling. *Plant Physiology* 132: 606-617.
684 24. Rogers EE, Glazebrook J, Ausubel FM (1996) Mode of action of the
685 *Arabidopsis thaliana* phytoalexin camalexin and its role in *Arabidopsis*-
686 pathogen interactions. *Molecular Plant-Microbe Interactions* 9: 748-757.
687 25. Zhou N, Tootlea TL, Glazebrook J (1999) *Arabidopsis PAD3*, a gene required for
688 camalexin biosynthesis, encodes a putative cytochrome P450 monooxygenase. *The*
689 *Plant Cell* 11: 2419-2428.
690 26. Lawrence CB, Mitchell TK, Craven KD, Chom Y, Cramer Jr RA, Kim K–H (2008)
691 At Death's Door: Alternaria Pathogenicity Mechanisms. *Plant Pathology Journal*
692 24, 101-111.
693 27. Cho Y, Ohm RA, Grigoriev IV, Srivastava A (2013) Fungal-specific transcription
694 factor AbPf2 activates pathogenicity in Alternaria brassicicola. *The Plant Journal*
695 75: 498–514.

696 28. Flors V, Ton J, van Doorn R, Jakab G, Garcia-Agustin P, Mauch-Mani B (2008)
697 Interplay between JA, SA and ABA signalling during basal and induced resistance
698 against *Pseudomonas syringae* and *Alternaria brassicicola*. *The Plant Journal* 54:
699 81–92.
700 29. Lipka V, Dittgen J, Bednarek P, Bhat R, Wiermer M, Stein M, Landtag J, Brandt
701 W, Rosahl S, Scheel D, Llorente F, Molina A, Parker J, Somerville S, Schulze-
702 Lefert P (2005) Pre- and post-invasion defenses both contribute to nonhost
703 resistance in *Arabidopsis*. *Science* 310: 1180-1183.
704 30. Hiruma K, Nishiuchi T, Kato K, Bednarek P, Okuno T, Schulze-Lefert P,
705 Takano Y (2011) *Arabidopsis* ENHANCED DISEASE RESISTANCE 1 is
706 required for pathogen-induced expression of plant defensins in nonhost resistance,
707 and acts through interference of MYC2-mediated repressor function. *The Plant*
708 *Journal* 67: 980–992.
709 31. Kagan IA, Hammerschmidt R (2002) *Arabidopsis* ecotype variability in camalexin
710 production and reaction to infection by *Alternaria brassicicola*. *Journal of*
711 *Chemical Ecology* 23: 2121-2140.
712 32. Stukkens Y, Bultreys A, Grec S, Trombik T, Vanham D, Boutry M (2005)
713 NpPDR1, a pleiotropic drug resistance-type ATP-binding cassette transporter from
714 *Nicotiana plumbaginifolia*, plays a major role in plant pathogen defense. *Plant*
715 *Physiology* 139: 341–352.
716 33. Thomma BPHJ, Eggermont K, Penninckx IAMA, Mauch-Mani B, Vogelsang R,
717 Cammue BPA, Broekaert WF (1998) Separate jasmonate-dependent and
718 salicylate-dependent defense-response pathways in *Arabidopsis* are essential for
719 resistance to distinct microbial pathogens. *Proc Natl Acad Sci USA* 95: 15107–

720 15111.
721 34. Glazebrook J (2005) Contrasting mechanisms of defense against biotrophic and
722 necrotrophic pathogens. *Annu Rev Phytopathol* 43: 205-227.
723 35. Stein RJ, Waters BM (2012) Use of natural variation reveals core genes in the
724 transcriptome of iron-deficient *Arabidopsis thaliana* roots. *Journal of*
725 *Experimental Botany* 63: 1039–1055.
726 36. Barah P, Jayavelu ND, Rasmussen S, Nielsen HB, Mundy J, Bones AM (2013)
727 Genome-scale cold stress response regulatory networks in ten *Arabidopsis*
728 *thaliana* ecotypes. *BMC Genomics* 14: 722.
729 37. Cramer R A, Lawrence C B (2004) Identification of *Alternaria brassicicola* genes
730 expressed *in planta* during pathogenesis of *Arabidopsis thaliana*. *Fungal genetics*
731 *and Biology* 41: 115-128.
732 38. Langowski L, Ruzicka K, Naramoto S, Kleine-Vehn J, Friml J (2010) Trafficking
733 to the outer polar domain defines the root-soil interface. *Current Biology* 20: 904–
734 908.
735 39. Ružicka K, Strader LC, Bailly A, Yang H, Blakeslee J, Łangowski L, Nejedlá E,
736 Fujita H, Itoh H, Syono K, Hejátko J, Gray WM, Martinoia E, Geisler M, Bartel B,
737 Murphy AS, Friml J (2010) *Arabidopsis* PIS1 encodes the ABCG37 transporter of
738 auxinic compounds including the auxin precursor indole-3-butyric acid. *Proc Natl*
739 *Acad Sci USA* 107: 10749–10753.
740 40. Łangowski Ł, Wabnik K, Li H, Vanneste S, Naramoto S,Tanaka H, Friml J (2016)
741 Cellular mechanisms for cargo delivery and polarity maintenance at different polar
742 domains in plant cells. *Cell Discovery* 2: 16018.
743 41. Glawischnig E, Hansen BG, Olsen CE, Halkier BA (2004) Camalexin is

744 synthesized from indole-3-acetaldoxime, a key branching point between primary
745 and secondary metabolism in *Arabidopsis*. *Proc Natl Acad Sci USA*101: 8245–50.
746 42. Crouzet J, Trombik T, Fraysse AS, Boutry M (2006) Organization and function of
747 the plant pleiotropic drug resistance ABC transporter family. *FEBS Letters* 580:
748 1123–1130.
749 43. Jungwirth H, Kuchler K (2006) Yeast ABC transporters – A tale of sex, stress,
750 drugs and aging. *FEBS Letters* 580:1131–1138.
751 44. Zhao J, Robert L (1996) Coordinate regulation of the tryptophan biosynthetic
752 pathway and indolic phytoalexin accumulation in *Arabidopsis*. *The Plant Cell* 8:
753 2235-2244.
754 45. Stefanato FL, Abou-Mansour E, Buchala A, Kretschmer M, Mosbach A, Hahn M,
755 Bochet G, Métraux J-P, Schoonbeek H-J (2009) The ABC transporter BcatrB
756 from *Botrytis cinerea* exports camalexin and is a virulence factor on *Arabidopsis*
757 *thaliana. The Plant Journal* 58: 499-510.
758 46. Bednarek P, Piślewska-Bednarek M, Svatoš A, Schneider B, Doubský J,
759 Mansurova M, Humphry M, Consonni C, Panstruga R, Sanchez-Vallet A, Molina
760 A, Schulze-Lefert P (2009) A Glucosinolate Metabolism Pathway in Living Plant
761 Cells Mediates Broad-Spectrum Antifungal Defense. *Science* 323:101-106.
762 47. Mysore KS, Ryu C–M (2004) Nonhost resistance: how much do we know? *Trends*
763 *in Plant science* 9: 97-104.
764 48. Consonni C, Bednarek P, Humphry M, Francocci F, Ferrari S, Harzen A, Themaat
765 EVLV, Panstruga R (2010) Tryptophan-Derived Metabolites Are Required for
766 Antifungal Defense in the *Arabidopsis mlo2* Mutant. *Plant Physiology* 152: 1544–
767 1561.

768 49. Egusa M, Miwa T, Kaminaka H, Takano Y, Kodama M (2013) Nonhost
769 resistance of *Arabidopsis thaliana* against *Alternaria alternata* involves both pre-
770 and post-invasive defenses but is collapsed by AAL-toxin in the absence of *LOH2*.
771 *Phytopathology* 103: 733-40.
772 50. Lazniewska J, Macioszek VK, Lawrence CB, Kononowicz AK (2010) Fight to the
773 death: *Arabidopsis thaliana* defense response to fungal necrotrophic pathogens.
774 *Acta Physiol Plant* 32: 1-10.
775 51. Nowicki M, Nowakowska M, Niezgoda A, Kozik E (2012) Alternaria black spot
776 of crucifers: Symptoms, importance of disease, and perspectives of resistance
777 breeding. *Vegetable Crops Research Bulletin,Versita, Warsaw,*
778 *Poland* doi:10.2478/v10032-012-0001-6.
779 52. Kumar D, Maurya N, Bharati YK, Kumar A, Kumar K, Srivastava K, Chand G,
780 Kushwaha C, Singh SK, Mishra R K, Kumar A (2014) Alternaria blight of oilseed
781 Brassicas: A comprehensive. *African Journal of Microbiology Research* 8: 2816-
782 2829.
783 53. Choi J, Huh SU, Kojima M, Sakakibara H, Paek K–H, Hwang I (2010) The
784 Cytokinin-Activated Transcription Factor ARR2 Promotes Plant Immunity via
785 TGA3/NPR1-dependent Salicylic Acid Signaling in *Arabidopsis*. *Dev Cell* 19 (2):
786 284-295.
787 54. Gachon C, Saindrenan P (2004) Real-time PCR monitoring of fungal development
788 in *Arabidopsis thaliana* infected by *Alternaria brassicicola* and *Botrytis cinerea.*
789 *Plant Physiology and Biochemistry* 42: 367–371.
790 55. Glazebrook J, Ausubel FM (1994) Isolation of phytoalexin-deficient mutants of
791 *Arabidopsis thaliana* and characterization of their interactions with bacterial

792 pathogens. *Proc Natl Acad Sci USA* 91: 8955-8959.
793 56. Savatin DV, Bisceglia NG, Gravino M, Fabbri C, Pontiggia D, Mattei B (2015)
794 Camalexin quantification in leaves infected with *B. cinerea*. *Bio Protocols* 5(2):
795 e1379. DOI: 10.21769. 1379.
796 57. Ohno R, Kadota Y, Fujii S, Sekine M, Umeda M, Kuchitsu K (2011) Cryptogein-
797 induced cell cycle arrest at G2 phase is associated with inhibition of cyclin-
798 dependent kinases, suppression of expression of cell cycle-related genes and
799 protein degradation in synchronized Tobacco BY2 Cells. *Plant Cell Physiology* 52:
800 922–932.
801 58. Mengiste T, Chen X, Salmeron JM, Dietrich RA (2003) The *BOS1* gene encodes
802 an R2R3MYB transcription factor protein that is required for biotic and abiotic
803 stress responses in *Arabidopsis*. *The Plant Cell* 15: 2551–2565.
804 59. Grubb CD, Gross HB, Chen DL, Abel S (2002) Identification
805 of *Arabidopsis* mutants with altered glucosinolate profiles based on isothiocyanate
806 bioactivity. *Plant Science* 162: 143–152.
807

808 **Figure Legends**

809 **Figure 1. Sclareol sensitive phenotype of *atabcg34* knockout plants.**

810 (A) *atabcg34* mutants (*ko-1, ko-2*) exhibit enhanced sclareol sensitivity compared to the
811 wild type. Plants were grown on ½ MS-agar plates in the absence (Control) or presence of
812 65 μM sclareol for two weeks.

813 (B) Sclareol tolerance was restored in complementation lines (C1-C3) expressing
814 *ABCG34pro:sGFP:ABCG34* in the *ko-1* background. Plants were grown on ½ MS-agar
815 plates without (Control) or with supplementation of 65 μM sclareol for two weeks. Scale

816 bar = 1 cm.

817 (C-D) Plant growth quantified by measuring fresh weight (C) and the longest root length
818 (D) of 2-week-old plants. Results are mean values (±SE) of three independent experiments
819 with three replicates each. Different lowercase letters indicate that the means are
820 significantly different between genotypes or treatments (Tukey's HSD test; $p<0.01$; N=3).

821

822 **Figure 2. AtABCG34 is required for resistance to *A. brassicicola*.**

823 (A-B) Disease symptoms of *atabcg34* mutants (*ko-1*, *ko-2*) and complementation lines
824 (C1-C3) on intact plants (2 weeks post inoculation; a) and detached leaves (5 days post
825 inoculation; b). Scale bar = 5 mm

826 (C) Fungal growth, as determined by amplification of the *A. brassicicola Cutinase* A (*Ab*)
827 gene relative to the *A. thaliana α shaggy kinase* (*At*) gene by qPCR at 5 dpi with *A.*
828 *brassicicola* (5 X 10^5 spores/ml). Graph represents mean values (±SE) of three biological
829 replicates with at least 21 disease lesions. Different characters indicate that the means are
830 significantly different between the genotypes (Tukey's HSD test, $p<0.01$; N=3).

831

832 **Figure 3. Expression profile after treatment with MeJA, SA and *A. brassicicola* and**
833 **polar localization of AtABCG34.**

834 (A-C) Time-dependent transcript level changes of *AtABCG34* in mature leaves treated with
835 50 µM MeJA (A), 1 mM SA (B) and *A. brassicicola* (5 X 10^5 spores/ml; C), quantified
836 relative to that of *AtACTIN7*. Data represent mean values (±SE) of three independent
837 experiments. Different lowercase letters indicate that the means are significantly different
838 (Tukey's HSD test, $p<0.01$; N=3).

839 (D-F) Plasma membrane localization of *ABCG34pro:sGFP:ABCG34* expressed in the *ko-1*

840 mutant at the epidermal cells of the mature rosette leaves (D). The images were taken at a
841 higher gain than were those in G. Polar localization of sGFP:ABCG34 in transverse
842 sections of mature leaf at the adaxial (upper panel) and abaxial (lower panel) surface (E)
843 and root (F). FM4-64 (10 µM) was used as a plasma membrane marker. Scale bar = 10 µm.
844 (G-H) Increase in GFP fluorescence of *ABCG34pro:sGFP:ABCG34* expressing in the
845 epidermal cells of leaves inoculated with *A. brassicicola* (5 X 10^5 spores/ml) observed at 6,
846 18, and 24 hpi (G) Scale bar = 70 µm . Fungal hyphae (white) were stained with calcoflour
847 white stain, ap: appressorium. In H, sGFP fluorescence intensity was quantified and
848 normalized to that from mock at 6 hpi, which was set to 1, using ImageJ, from photographs
849 as shown in G. Different lowercase letters indicate that the means are significantly
850 different (Tukey's HSD test, $p<0.05$; n=10).
851
852 **Figure 4. AtABCG34 mediates secretion of camalexin to the leaf surface.**
853 (A) Surface camalexin measured from whole rosettes of the wild type, *atabcg34* lines (*ko-1,*
854 *ko-2*), complementation lines (C1-C3), and overexpression lines (OE1-OE3) expressing
855 *35Spro:sGFP:ABCG34* in the wild-type background at 24 hpi of *A. brassicicola* (5 X 10^5
856 spores/ml). Graph represents mean values (±SE) from 5 different experiments with at least
857 6 rosettes per genotype per experiment. Different lowercase letters indicate that the means
858 are significantly different between genotypes (Tukey's HSD test, $p<0.01$; N=5).
859 (B) Total camalexin measured from the *A. thaliana* whole rosette of the wild type and
860 *atabcg34* (*ko-1*, *ko-2*) mutants at 24 hpi of *A. brassicicola*. Graphs represent mean values
861 (±SE) from 5 different experiments with at least 6 rosettes per genotype, per time point and
862 per experiment. Different lowercase letters indicate that the means are significantly
863 different between genotypes or time points (Tukey's HSD test, $p<0.01$; N=5).

(C) Photographs of disease symptoms of wild-type, *atabcg34-1* mutants and AtABCG34 overexpression lines (OE1-OE3) on detached leaves (top panels) and intact plants (bottom panels) taken at 3 and 14 dpi of *A. brassicicola,* respectively. Scale bar = 5 mm.

(D-E) Lesion diameter (D; N=3) and *A. brassicicola* growth quantified by amplification of the *A. brassicicola Cutinase* A (*Ab*) gene relative to the *A. thaliana α shaggy kinase* (*At*) gene by qPCR (E; N=3). Graph represents mean values (±SE) from three biological experiments with at least 15 leaves per genotype and experiment. Different lowercase letters indicate that the means are significantly different between genotypes (Tukey's HSD test, $p<0.01$).

Figure 5. Camalexin toxicity assay in *A. thaliana* and BY2 cells.

(A) Photographs of cell death in 3- to 4-week-old plants using Evans blue staining 24 h after treatment with DMSO (1%; top), camalexin (1 mg/ml; middle), or *A. brassicicola* (5 X 10^5 spores/ml; bottom). The experiment was repeated four independent times with similar results (N=4). Scale bar = 5 mm.

(B) BY2 cells expressing *35Spro:sGFP* (EV; top) and *$35S_{pro}$:sGFP:ABCG34* (ABCG34-1 and ABCG34-2; center and bottom). Merged indicates co-localization with red fluorescence of FM4-64 (10 μM), plasma membrane marker. Scale bar = 20 μm.

(C) Camalexin-induced BY2 cell death expressing EV or AtABCG34. A six-day-old culture of BY2 cells was treated with either DMSO (0.05%) or camalexin (250 μM) and cell death was analyzed by Evans blue staining 24 h after treatment.

(D) Camalexin-induced growth inhibition of BY2 cells. A three-day-old culture of BY2 cells was treated with either DMSO (0.01%) or camalexin (50 μM) and the optical density was measured at 4 days after treatment at 600 nm.

888 Graphs represent mean values (±SE) of three independent experiments. Different
889 lowercase letters indicate that the means are significantly different (Tukey's HSD test,
890 $p<0.01$; N=3).
891
892 **Figure 6. AtABCG34 is required for pre-invasion resistance to *A. brassicicola*.**
893 (A-B) Penetration sites of various lines of *A. thaliana* leaves infected with *A. brassicicola.*
894 Callose deposited at the penetration sites was stained with aniline blue at 24 hpi (A; scale
895 bar = 50 μm). Number of penetration sites was counted (B). Data represent mean values
896 (±SE) of three independent experiments with at least 10 leaves per genotype and per
897 experiment. Different lowercase letters indicate that the means are significantly different
898 between genotypes (Tukey's HSD test, $p<0.01$; N=3).
899 (C) Microscopy images of *A. brassicicola* conidia and hyphae (Upper panel) and % of
900 germinated *A. brassicicola* conidia (Lower panel) on the leaves of wild-type and
901 AtABCG34-overexpressing plants. In the upper panel, bright field images (top) and
902 calcoflour white fluorescent images (bottom) of conidia and hyphae are shown. Scale bar =
903 50 μm. In the lower panel, percent germinated *A. brassicicola* conidia at 24 hpi is shown
904 (n=15).
905 (D) Transcript levels of *AtPDF1.2* after *A. brassicicola* or *B. cinerea* infection in the wild
906 type and *atabcg34* mutants. Graph represents mean values (±SE) of three replicates (N=3).
907 Different lowercase letters indicate that the means are significantly different between the
908 genotypes (Tukey's HSD test, $p<0.05$).
909
910 **Figure 7. *A. brassicicola* growth and *AtABCG34* expression levels in different**
911 **accessions and *AtABCG34* overexpression lines of *Arabidopsis*.**

(A) Disease symptoms in detached leaves. Photographs were taken at 5 dpi with *A. brassicicola* (5 X 10^5 spores/ml). Scale bar = 5 mm.

(B) Growth of *A. brassicicola*, as determined by amplification of the genomic *A. brassicicola Cutinase* A (*Ab*) and the genomic *A. thaliana α shaggy kinase* (*At*) by qPCR. Graph represents mean values (±SE) from three biological replicates with 27 lesions from 15 different plants (N=3).

(C) *AtABCG34* transcript levels in leaves of 3- to 4-week-old plants under control conditions. Graph represents mean values (±SE) from three biological replicates using qRT-PCR. Different lowercase letters indicate that the means are significantly different between the accessions (Tukey's HSD test, $p<0.05$; N=3).

(D-E) Regression analysis for the correlation between *AtABCG34* expression (mean ±SE) and *A. brassicicola* growth (logarithmic transformed geometric mean ±SE) in 12 different accessions (D) and in 12 different accessions and three overexpression lines (OE1–OE3; E).

Figure 8. Working model for the function of AtABCG34.

Inoculation of *A. thaliana* leaves with *A. brassicicola* induces the expression of *AtABCG34,* the camalexin biosynthesis gene PAD3, and JA signaling genes. JA also induces the expression of *AtABCG34* and *AtPDF1.2*. AtABCG34-mediated secretion of camalexin to the surface inhibits *A. brassicicola* growth in the wild type (solid red lines in the top panel). Reduced camalexin secretion and *AtPDF1.2* expression (small font) allow pathogen growth in the *atabcg34* mutant (broken red lines in the bottom panel). Orange circles represent camalexin. The chemical structure of camalexin is shown at the right.

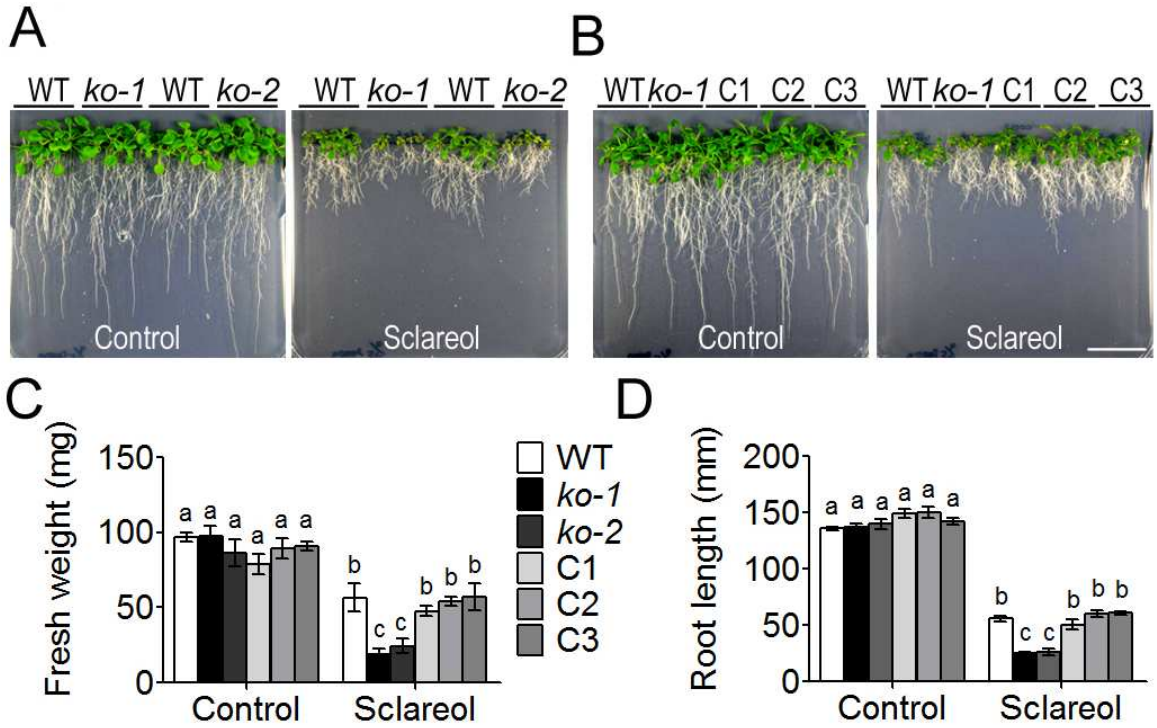

Figure 1. Sclareol sensitive phenotype of *atabcg34* knockout plants.

(A) *atabcg34* mutants (*ko-1, ko-2*) exhibit enhanced sclareol sensitivity compared to the wild type. Plants were grown on ½ MS-agar plates in the absence (Control) or presence of 65 µM sclareol for two weeks.

(B) Sclareol tolerance was restored in complementation lines (C1-C3) expressing *ABCG34pro:sGFP:ABCG34* in the *ko-1* background. Plants were grown on ½ MS-agar plates without (Control) or with supplementation of 65 µM sclareol for two weeks. Scale bar = 1 cm.

(C-D) Plant growth quantified by measuring fresh weight (C) and the longest root length (D) of 2-week-old plants. Results are mean values (±SE) of three independent experiments with three replicates each. Different lowercase letters indicate that the means are significantly different between genotypes or treatments (Tukey's HSD test; $p<0.01$; N=3).

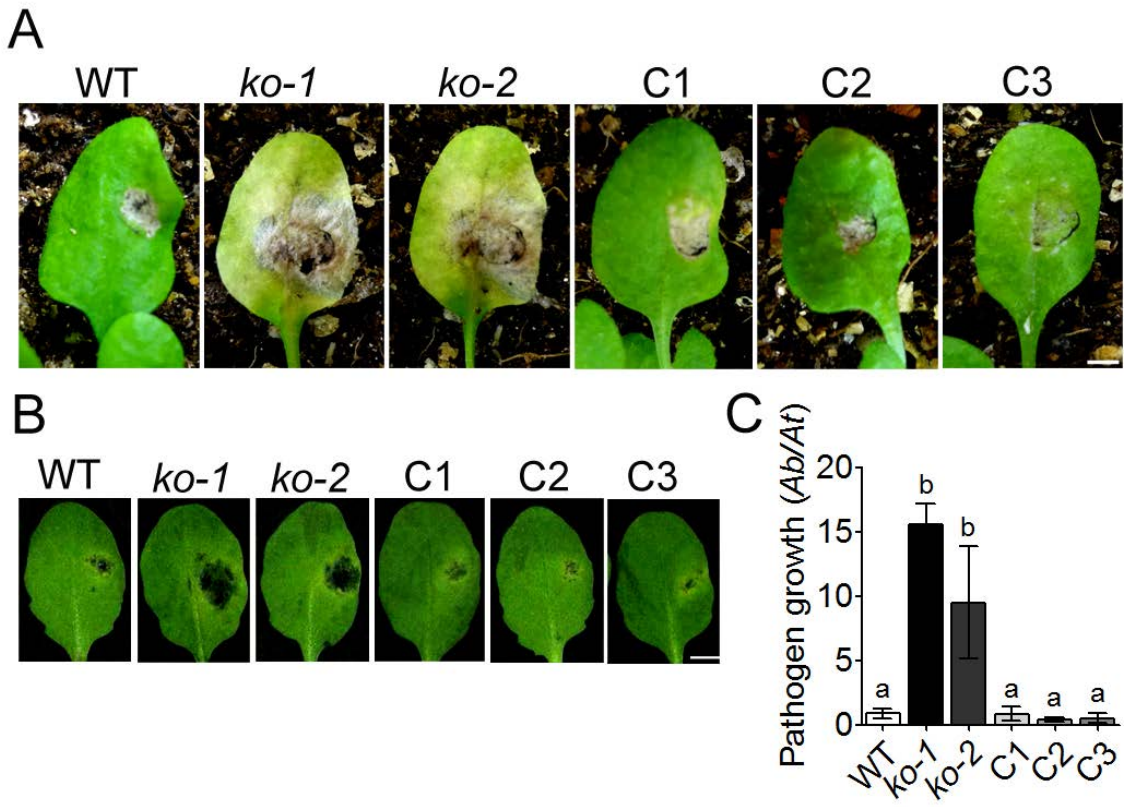

Figure 2. AtABCG34 is required for resistance to *A. brassicicola*.

(A-B) Disease symptoms of *atabcg34* mutants (*ko-1*, *ko-2*) and complementation lines (C1-C3) on intact plants (2 weeks post inoculation; a) and detached leaves (5 days post inoculation; b). Scale bar = 5 mm

(C) Fungal growth, as determined by amplification of the *A. brassicicola Cutinase* A (*Ab*) gene relative to the *A. thaliana α shaggy kinase* (*At*) gene by qPCR at 5 dpi with *A. brassicicola* (5 X 10^5 spores/ml). Graph represents mean values (±SE) of three biological replicates with at least 21 disease lesions. Different characters indicate that the means are significantly different between the genotypes (Tukey's HSD test, $p<0.01$; N=3).

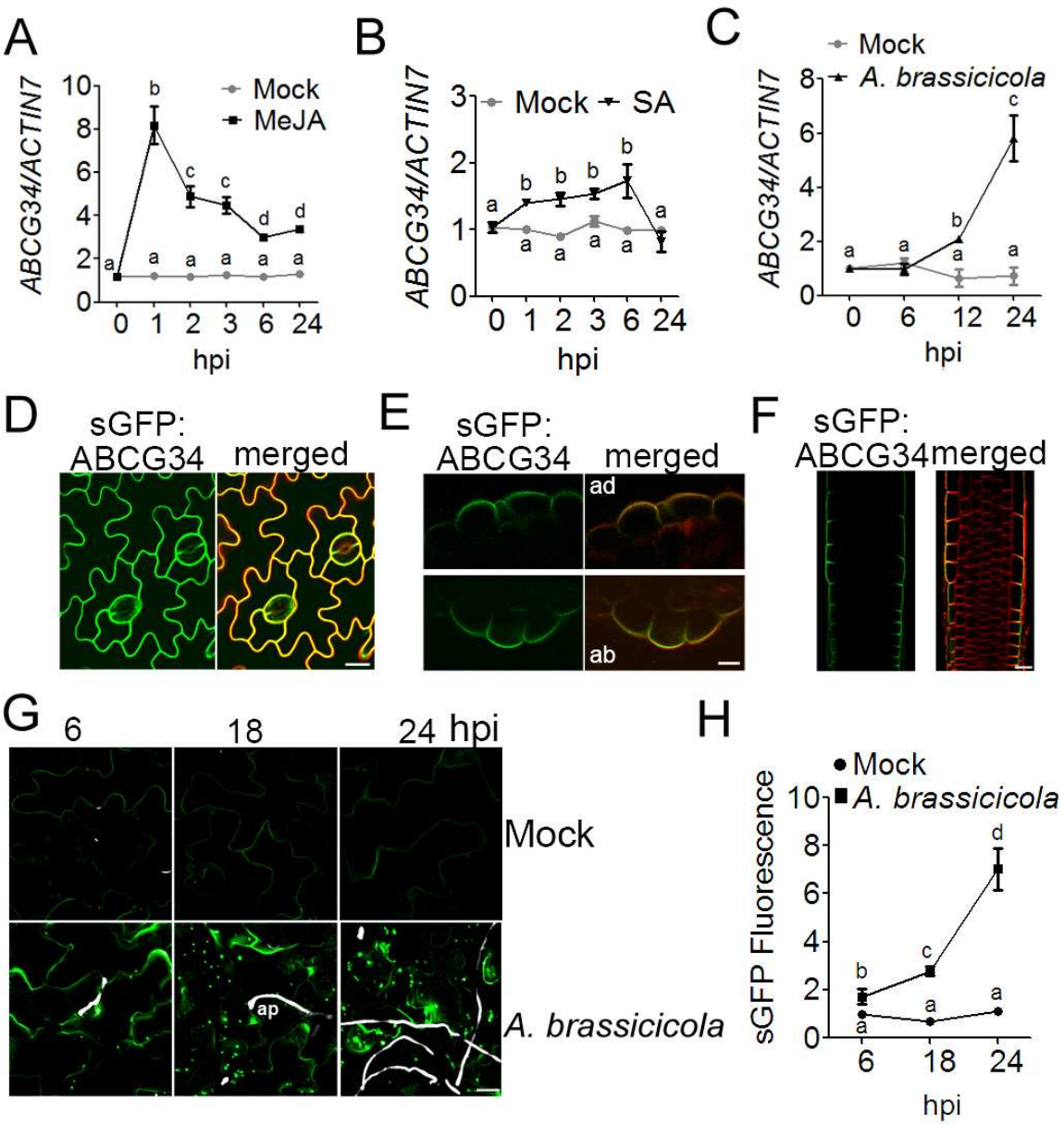

Figure 3. Expression profile after treatment with MeJA, SA and *A. brassicicola* and polar localization of AtABCG34.

(A-C) Time-dependent transcript level changes of *AtABCG34* in mature leaves treated with 50 µM MeJA (A), 1 mM SA (B) and *A. brassicicola* (5 X 10^5 spores/ml; C), quantified relative to that of *AtACTIN7*. Data represent mean values (±SE) of three independent experiments. Different lowercase letters indicate that the means are significantly different (Tukey's HSD test, $p<0.01$; N=3).

(D-F) Plasma membrane localization of *ABCG34pro:sGFP:ABCG34* expressed in the *ko-1* mutant at the epidermal cells of the mature rosette leaves (D). The images were taken at a higher gain than were those in G. Polar localization of sGFP:ABCG34 in transverse sections of mature leaf at the adaxial (upper panel) and abaxial (lower panel) surface (E) and root (F). FM4-64 (10 µM) was used as a plasma membrane marker. Scale bar = 10 µm.

(G-H) Increase in GFP fluorescence of *ABCG34pro:sGFP:ABCG34* expressing in the epidermal cells of leaves inoculated with *A. brassicicola* (5 X 10^5 spores/ml) observed at 6,

18, and 24 hpi (G) Scale bar = 70 µm . Fungal hyphae (white) were stained with calcoflour white stain, ap: appressorium. In H, sGFP fluorescence intensity was quantified and normalized to that from mock at 6 hpi, which was set to 1, using ImageJ, from photographs as shown in G. Different lowercase letters indicate that the means are significantly different (Tukey's HSD test, $p<0.05$; $n=10$).

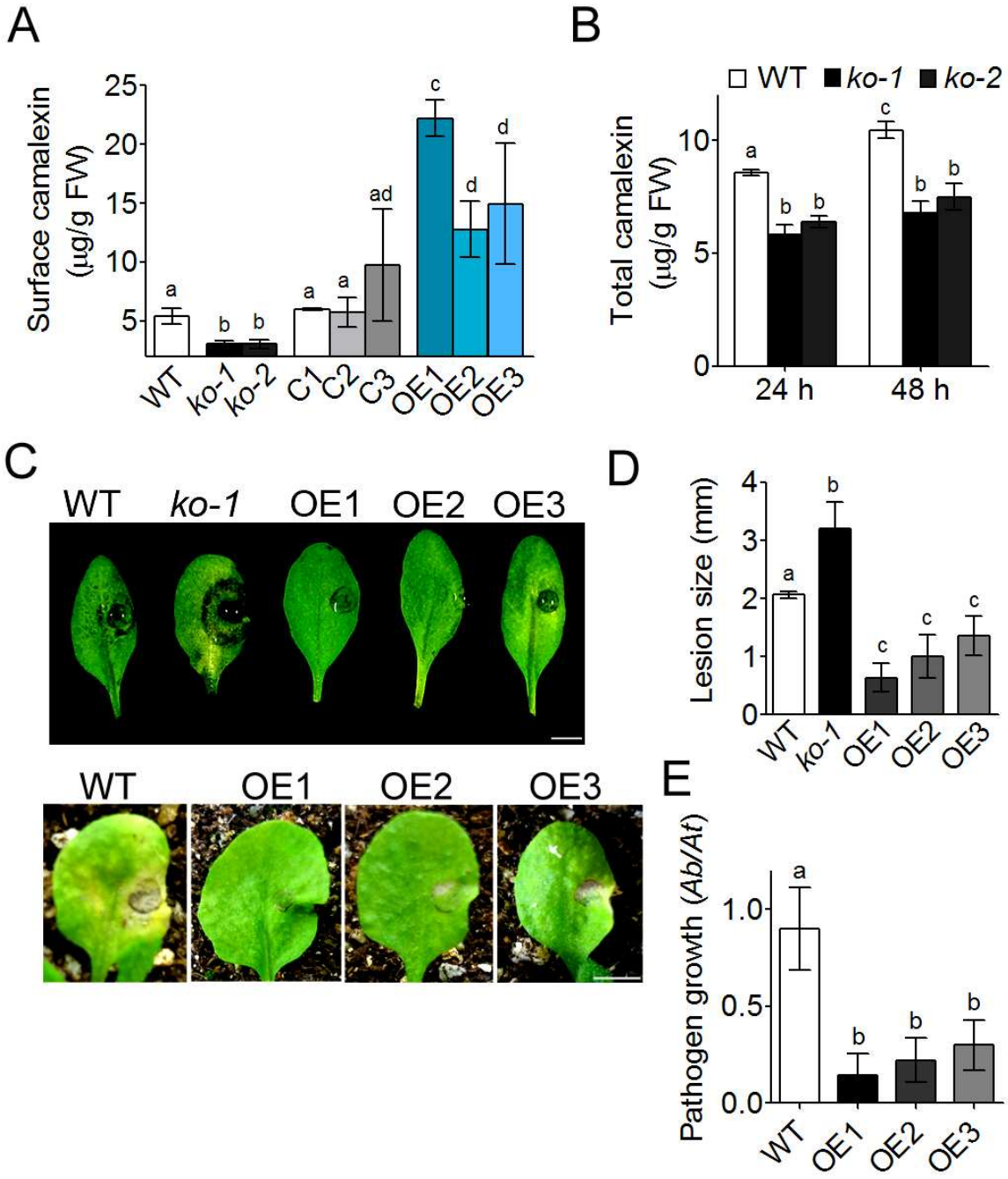

Figure 4. AtABCG34 mediates secretion of camalexin to the leaf surface.

(A) Surface camalexin measured from whole rosettes of the wild type, *atabcg34* lines (*ko-1, ko-2*), complementation lines (C1-C3), and overexpression lines (OE1-OE3) expressing *35Spro:sGFP:ABCG34* in the wild-type background at 24 hpi of *A. brassicicola* (5 X 10^5 spores/ml). Graph represents mean values (±SE) from 5 different experiments with at least 6 rosettes per genotype per experiment. Different lowercase letters indicate that the means are significantly different between genotypes (Tukey's HSD test, $p<0.01$; N=5).

(B) Total camalexin measured from the *A. thaliana* whole rosette of the wild type and *atabcg34* (*ko-1*, *ko-2*) mutants at 24 hpi of *A. brassicicola*. Graphs represent mean values (±SE) from 5 different experiments with at least 6 rosettes per genotype, per time point and

per experiment. Different lowercase letters indicate that the means are significantly different between genotypes or time points (Tukey's HSD test, $p<0.01$; N=5).
(C) Photographs of disease symptoms of wild-type, *atabcg34-1* mutants and AtABCG34 overexpression lines (OE1-OE3) on detached leaves (top panels) and intact plants (bottom panels) taken at 3 and 14 dpi of *A. brassicicola,* respectively. Scale bar = 5 mm.
(D-E) Lesion diameter (D; N=3) and *A. brassicicola* growth quantified by amplification of the *A. brassicicola Cutinase* A (*Ab*) gene relative to the *A. thaliana α shaggy kinase* (*At*) gene by qPCR (E; N=3). Graph represents mean values (±SE) from three biological experiments with at least 15 leaves per genotype and experiment. Different lowercase letters indicate that the means are significantly different between genotypes (Tukey's HSD test, $p<0.01$).

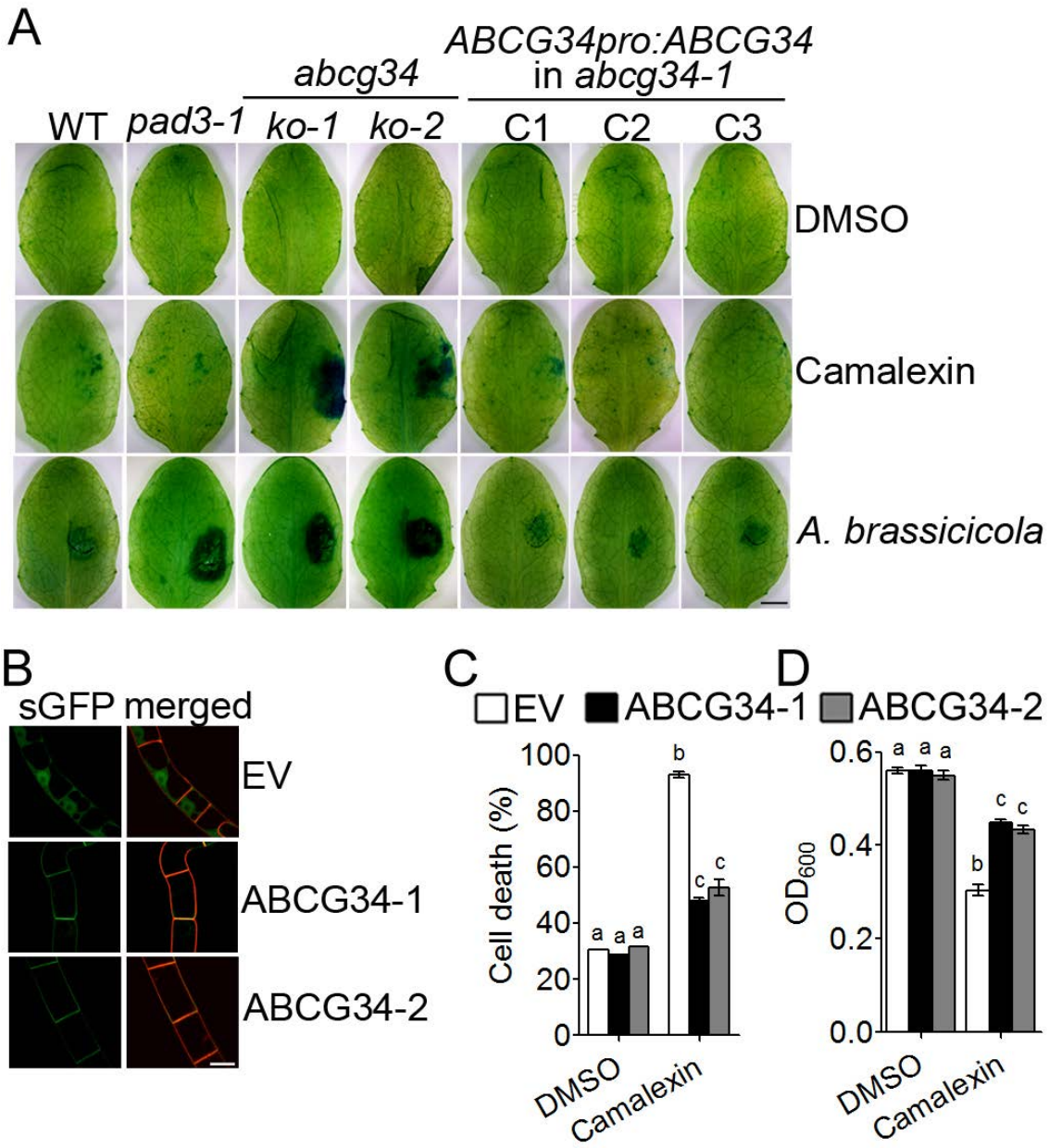

Figure 5. Camalexin toxicity assay in *A. thaliana* and BY2 cells.

(A) Photographs of cell death in 3- to 4-week-old plants using Evans blue staining 24 h after treatment with DMSO (1%; top), camalexin (1 mg/ml; middle), or *A. brassicicola* (5 X 10^5 spores/ml; bottom). The experiment was repeated four independent times with similar results (N=4). Scale bar = 5 mm.

(B) BY2 cells expressing *35Spro:sGFP* (EV; top) and *$35S_{pro}$:sGFP:ABCG34* (ABCG34-1 and ABCG34-2; center and bottom). Merged indicates co-localization with red fluorescence of FM4-64 (10 μM), plasma membrane marker. Scale bar = 20 μm.

(C) Camalexin-induced BY2 cell death expressing EV or AtABCG34. A six-day-old culture of BY2 cells was treated with either DMSO (0.05%) or camalexin (250 μM) and cell death was analyzed by Evans blue staining 24 h after treatment.

(D) Camalexin-induced growth inhibition of BY2 cells. A three-day-old culture of BY2 cells was treated with either DMSO (0.01%) or camalexin (50 μM) and the optical density was

measured at 4 days after treatment at 600 nm.
Graphs represent mean values (±SE) of three independent experiments. Different lowercase letters indicate that the means are significantly different (Tukey's HSD test, $p<0.01$; N=3).

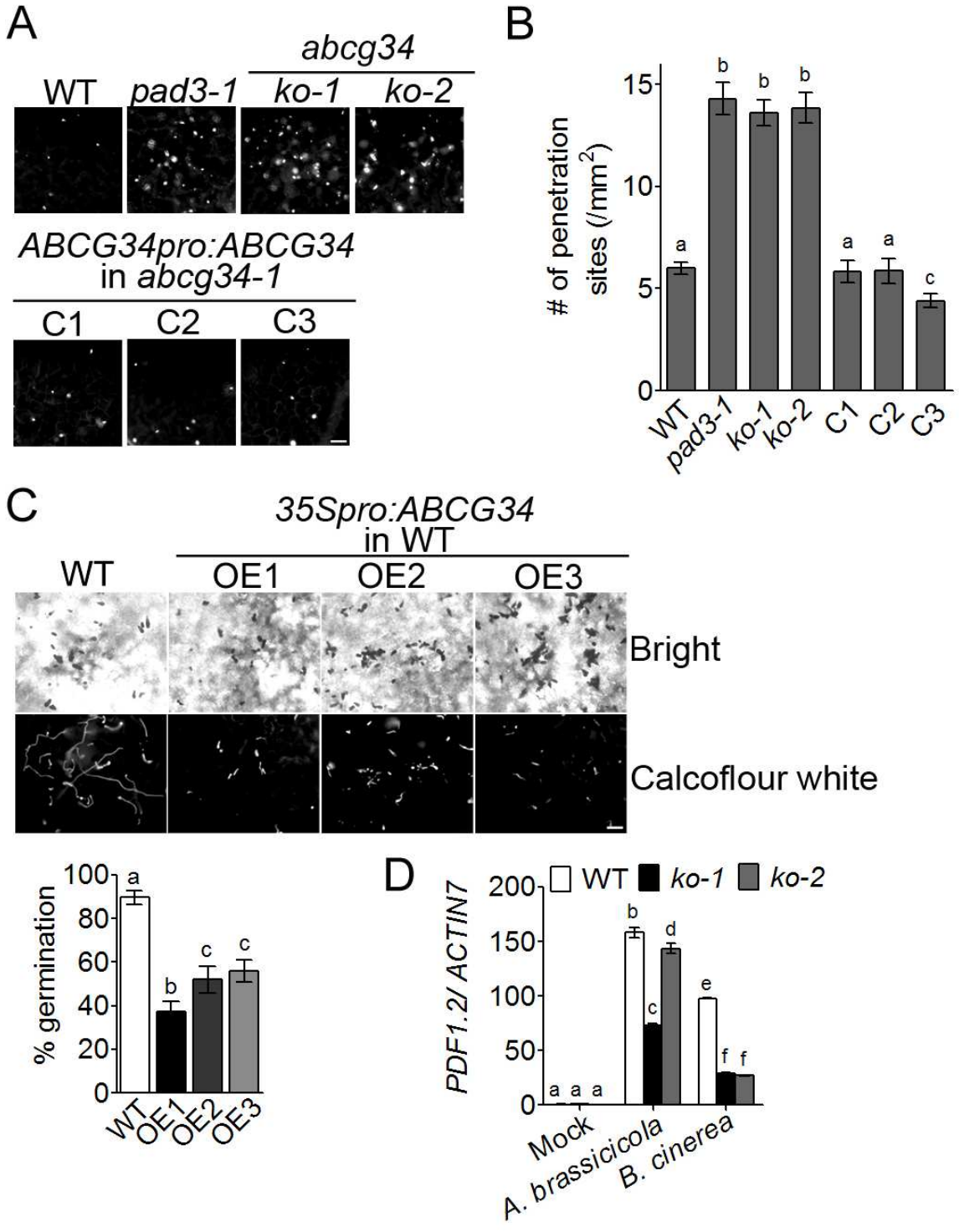

Figure 6. AtABCG34 is required for pre-invasion resistance to *A. brassicicola*.
(A-B) Penetration sites of various lines of *A. thaliana* leaves infected with *A. brassicicola.* Callose deposited at the penetration sites was stained with aniline blue at 24 hpi (A; scale bar = 50 µm). Number of penetration sites was counted (B). Data represent mean values (±SE) of three independent experiments with at least 10 leaves per genotype and per experiment. Different lowercase letters indicate that the means are significantly different between genotypes (Tukey's HSD test, $p<0.01$; N=3).

(C) Microscopy images of *A. brassicicola* conidia and hyphae (Upper panel) and % of germinated *A. brassicicola* conidia (Lower panel) on the leaves of wild-type and AtABCG34-overexpressing plants. In the upper panel, bright field images (top) and calcoflour white fluorescent images (bottom) of conidia and hyphae are shown. Scale bar = 50 µm. In the lower panel, percent germinated *A. brassicicola* conidia at 24 hpi is shown (n=15).
(D) Transcript levels of *AtPDF1.2* after *A. brassicicola* or *B. cinerea* infection in the wild type and *atabcg34* mutants. Graph represents mean values (±SE) of three replicates (N=3). Different lowercase letters indicate that the means are significantly different between the genotypes (Tukey's HSD test, $p<0.05$).

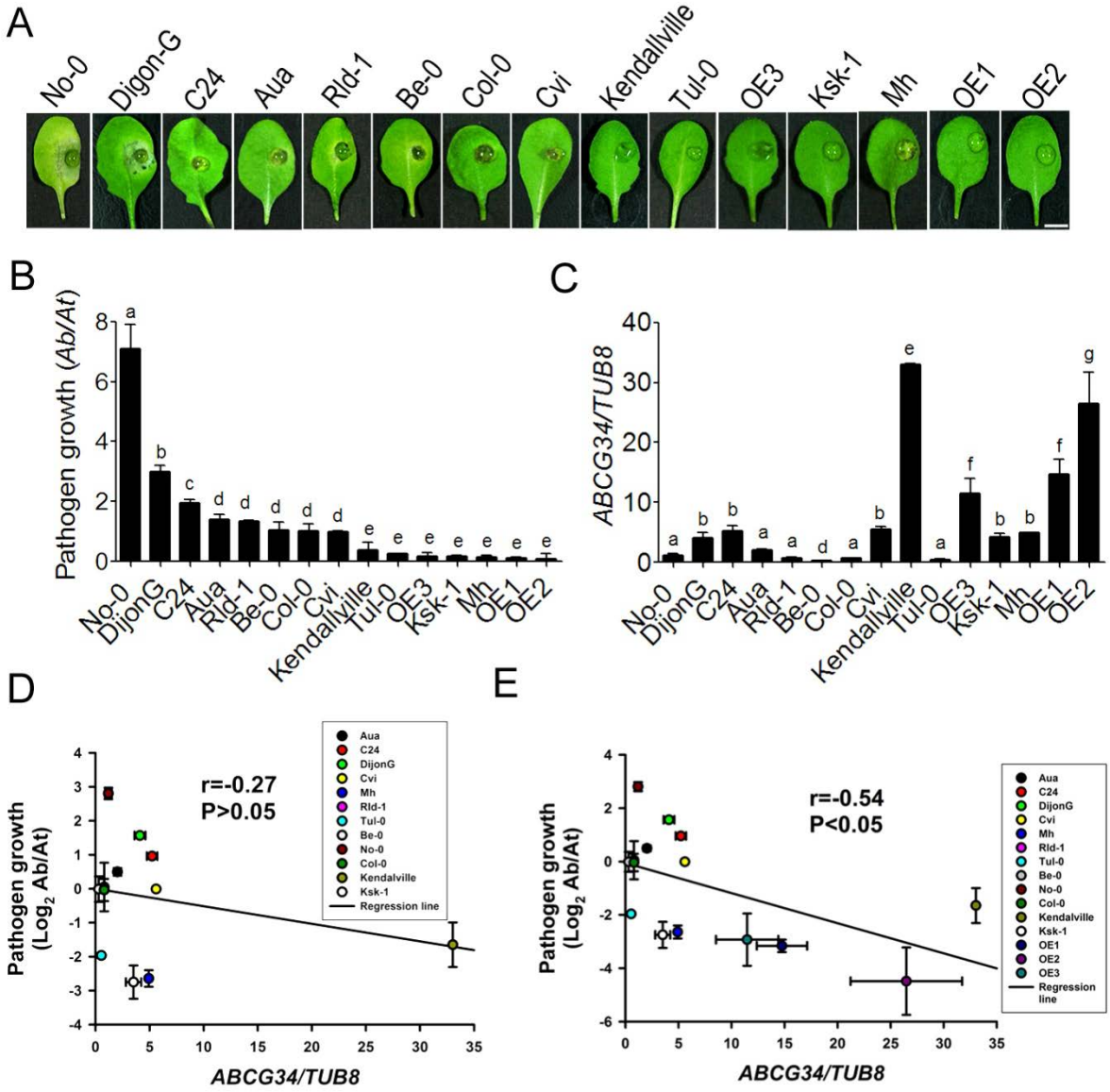

Figure 7. *A. brassicicola* growth and *AtABCG34* expression levels in different accessions and *AtABCG34* overexpression lines of *Arabidopsis*.

(A) Disease symptoms in detached leaves. Photographs were taken at 5 dpi with *A. brassicicola* (5 X 10^5 spores/ml). Scale bar = 5 mm.

(B) Growth of *A. brassicicola*, as determined by amplification of the genomic *A. brassicicola Cutinase* A (*Ab*) and the genomic *A. thaliana α shaggy kinase* (*At*) by qPCR. Graph represents mean values (±SE) from three biological replicates with 27 lesions from 15 different plants (N=3).

(C) *AtABCG34* transcript levels in leaves of 3- to 4-week-old plants under control conditions. Graph represents mean values (±SE) from three biological replicates using qRT-PCR. Different lowercase letters indicate that the means are significantly different between the accessions (Tukey's HSD test, $p<0.05$; N=3).

(D-E) Regression analysis for the correlation between *AtABCG34* expression (mean ±SE) and *A. brassicicola* growth (logarithmic transformed geometric mean ±SE) in 12 different accessions (D) and in 12 different accessions and three overexpression lines (OE1–OE3; E).

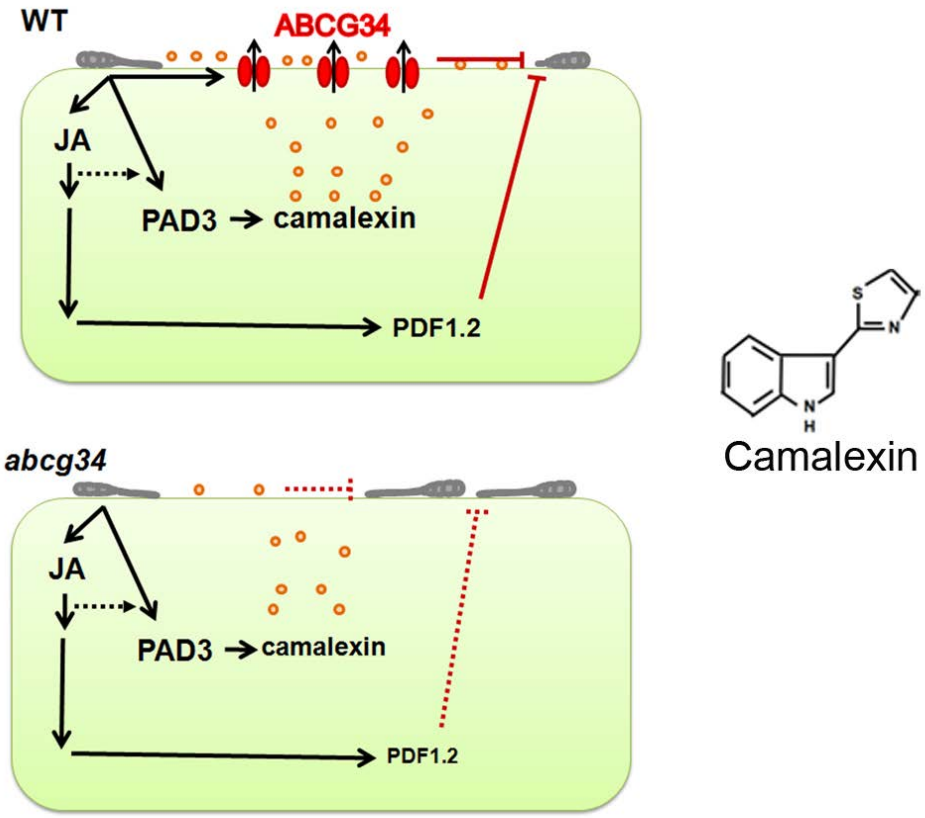

Figure 8. Working model for the function of AtABCG34.

Inoculation of *A. thaliana* leaves with *A. brassicicola* induces the expression of *AtABCG34,* the camalexin biosynthesis gene PAD3, and JA signaling genes. JA also induces the expression of *AtABCG34* and *AtPDF1.2*. AtABCG34-mediated secretion of camalexin to the surface inhibits *A. brassicicola* growth in the wild type (solid red lines in the top panel). Reduced camalexin secretion and *AtPDF1.2* expression (small font) allow pathogen growth in the *atabcg34* mutant (broken red lines in the bottom panel). Orange circles represent camalexin. The chemical structure of camalexin is shown at the right.

Supplementary Information

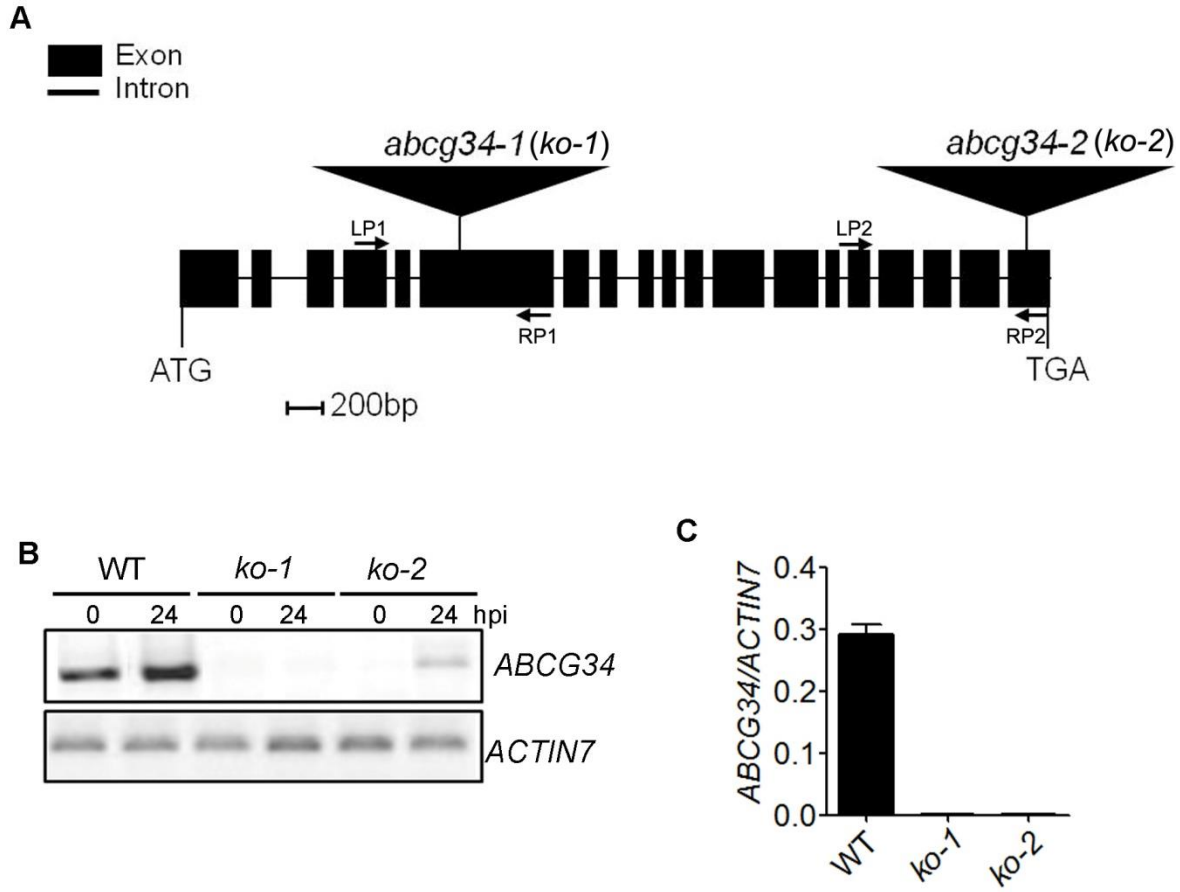

Supplementary Figure 1. Isolation of *atabcg34* knockout mutants.

(A) Structure of *AtABCG34* showing the positions of the T-DNA insertions. Exons and introns are indicated by black boxes and lines, respectively. The T-DNA insertion sites in the SAIL_5_G10 (*atabcg34-1*) and SALK_036087 (*atabcg34-2*) are indicated by flags.

(B) RT-PCR analysis of *AtABCG34* expression in seedlings inoculated (24 hpi) or not with *A. brassicicola* (5 X 10^5 spores/ml). Total RNA was extracted from 3- to 4-week-old wild-type (WT), *ko-1* (*atabcg34-1),* and *ko-2* (*atabcg34-2)* seedlings. *AtACTIN7* was used as a loading control. A low level of *AtABCG34* was induced in the *ko-2* mutant after inoculation with *A. brassicicola*.

(C) Graph represents mean values (±SE) of transcript levels of *AtABCG34* in the wild type and *abcg34* (*ko-1 and ko-2*) mutants, analyzed by qRT-PCR and normalized by *AtACTIN7* transcripts from three technical replicates (n=3).

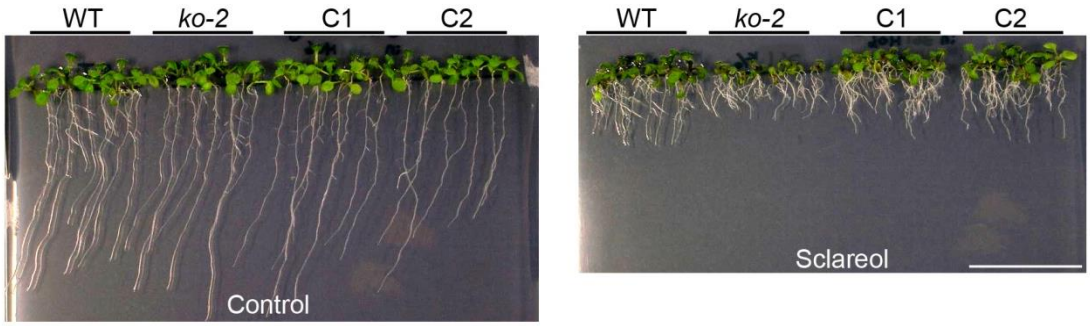

Supplementary Figure 2. The sclareol-sensitive phenotype of *atabcg34-2* is restored by AtABCG34 complementation.

The sclareol sensitivity of *abcg34-2* is restored by complementation of *ABCG34pro:sGFP:ABCG34* in the *atabcg34-2 (ko-2)* background (C1 and C2). Plants were grown for two weeks on ½ MS-agar plates in the absence (Control; left) or presence (right) of 65 µM sclareol (N=3). Scale bar = 1 cm.

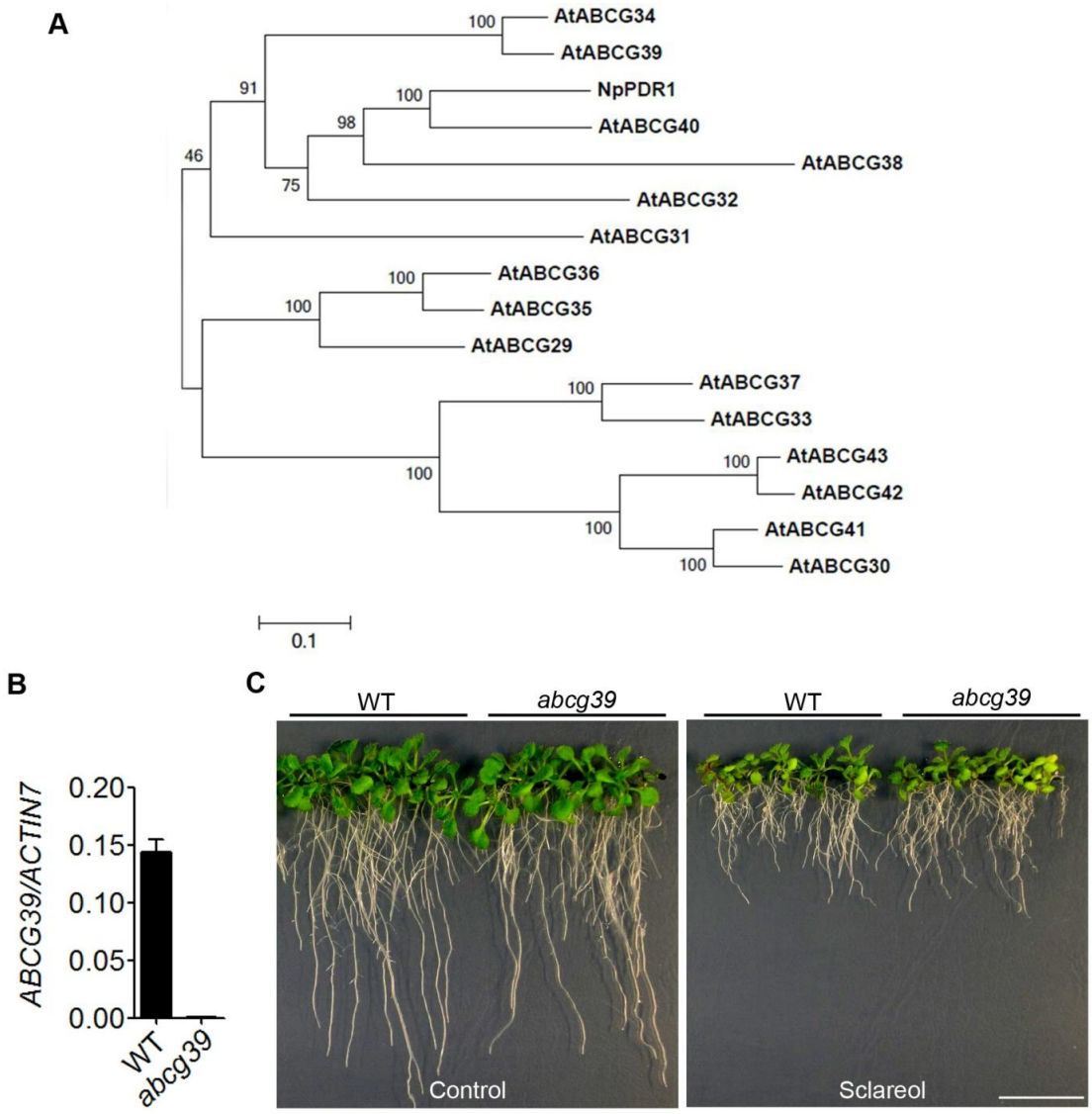

Supplementary Figure 3. Phylogenic tree of *A. thaliana* full-size ABCG proteins and growth of *atabcg39* mutants in sclareol containing media.

(A) Phylogenic tree of *A. thaliana* full-size ABCG (PDR) proteins produced using MEGA4 software. NpPDR1 clusters with AtABCG34, AtABCG39, and AtABCG40.

(B) qRT-PCR analysis of *AtABCG39* transcript. Graph represents mean values (±SE) of transcript levels of *AtABCG39* in the wild type and *atabcg39* mutant. *AtACTIN7* was used as an internal control (n=3).

(C) Growth of the *atabcg39* mutant compared to the wild type. Plants were grown on ½ MS-agar plates without (Control) or with supplementation with 65 µM sclareol for three weeks (N=3). Scale bar = 1 cm.

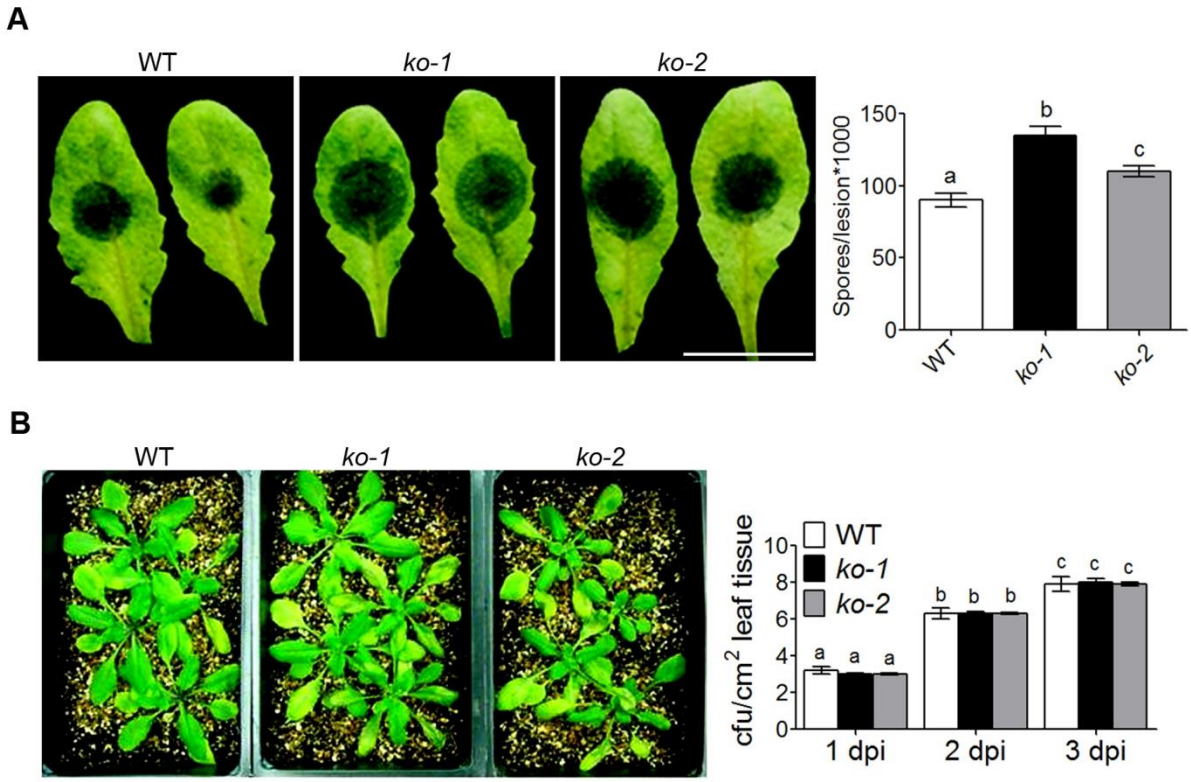

Supplementary Figure 4. AtABCG34 is required for resistance to *B. cinerea,* but not for *Pst* DC3000.

(A) Disease symptoms of *atabcg34* mutants (*ko-1*, *ko-2*) and the wild type on detached leaves after *B. cinerea* treatment. Photographs of the detached leaves (left) and graph represents mean values (±SE) of fungal growth, as determined by counting the spores at 5 dpi (right). n=14 for spore population (number per unit area). Scale bar = 1cm.

(B) The *atabcg34* mutants and wild-type plants exhibited no difference in sensitivity to *Pst* DC3000 (n=10). Photographs (left) and graph represents mean values (±SE) of bacterial growth at 4 dpi (right). cfu: colony forming units.

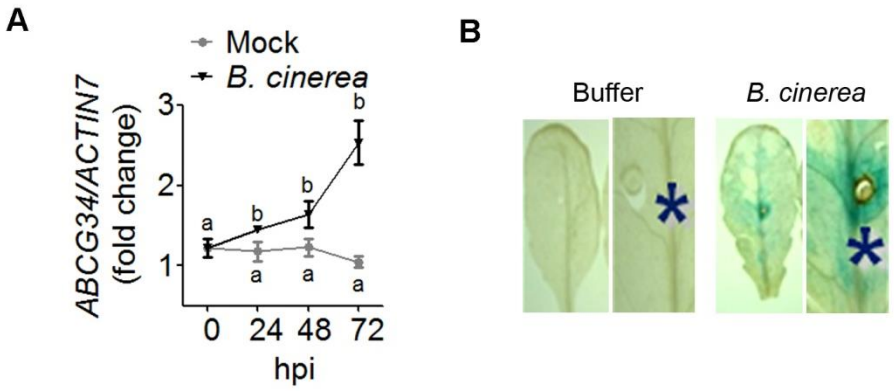

Supplementary Figure 5. Expression profile of *AtABCG34* after treatment with *B. cinerea*.

(A) Transcript level of *AtABCG34* after *B. cinerea* treatment. Transcript was analyzed by quantitative RT-PCR after mock or *B. cinerea* treatment at different time points. Data represent mean values (±SE) of three independent experiments (N=3). Different lowercase letters indicate that the means are significantly different (Tukey's HSD test, $p<0.01$).

(B) Leaves of 3-week-old *ABCG34*$_{pro}$*:GUS* expressing plants were inoculated with buffer or *B. cinerea.* Asterisks indicate the site of inoculation. A GUS assay was executed at 3 dpi. The leaves were punctured with needles before inoculation for efficient infection.

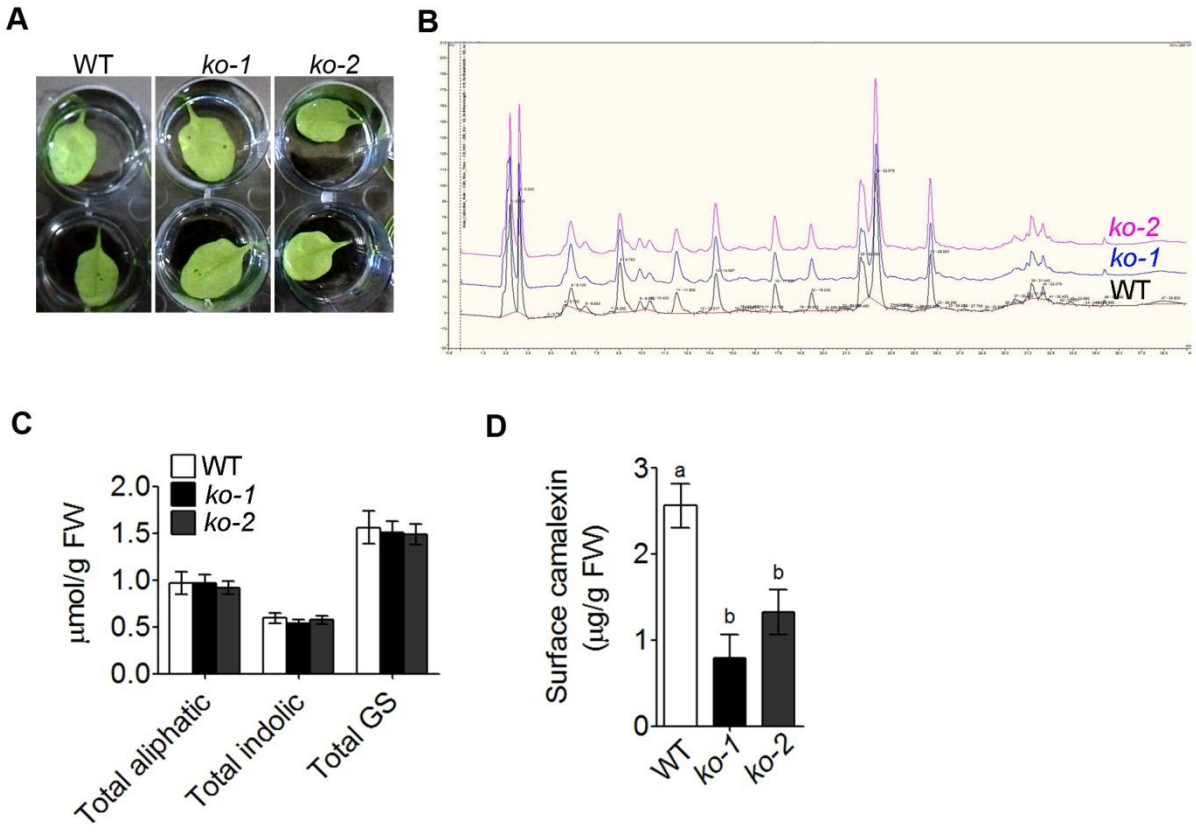

Supplementary Figure 6. At**ABCG34 is not required for cutin formation or for transport of glucosinolates and phenolic compounds.**

(A) Ethanol penetration assay for cuticle permeability. The leaves of 3-week-old wild-type and *atabcg34* mutants (*ko-1, ko-2*) were immersed in 100% ethanol and penetration was assessed after 5 min of immersion (N=3).

(B) Chromatogram of phenolics extracted from wild-type and *atabcg34* (*ko-1, ko-2*) mutant plants at 24 hpi with *B. cinerea*. The experiment was performed using four individuals per genotype (N=2).

(C) Glucosinolates measured from wild-type and *atabcg34* (*ko-1, ko-2*) mutants at 24 hpi with *A. brassicicola*. Graph represents (±SE) mean values of two independent experiments with three replicates each (N=2).

(d) Surface camalexin measured from whole rosettes of wild-type and *atabcg34* (*ko-1, ko-2*) mutant plants at 48 hpi of *A. brassicicola*. Graphs represent mean values (±SE) from five different experiments with at least six rosettes per genotype and experiment. Different

lowercase letters indicate that the means are significantly different between genotypes (Tukey's HSD test, $p<0.01$; N=5).

(d) Surface camalexin measured from whole rosettes of wild-type and *atabcg34* (*ko-1, ko-2*) mutant plants at 48 hpi of *A. brassicicola*. Graphs represent mean values (±SE) from five different experiments with at least six rosettes per genotype and experiment. Different lowercase letters indicate that the means are significantly different between genotypes (Tukey's HSD test, $p<0.01$; N=5).

Material and Methods:

Isolation of Knockouts

T-DNA insertion mutants of *atabcg34*, *atabcg39* and a point mutant of *atpad3-1* (25) were obtained from the *Arabidopsis* Biological Resource *Center*. T-DNA insertional mutants from the SAIL collection (*abcg34-1*), and the SALK institute (*abcg34-2*) were isolated by genotyping using a gene-specific primer and a T-DNA left border-specific primer. Total RNA was extracted from wild-type (WT), *abcg34-1,* and *abcg34-2* SALK_067836 (*abcg39*) seedlings and transcript levels were checked by RT-PCR and qRT-PCR using primers listed in Table S1.

Bacterial Disease Assay

The leaves of 4-week-old *A. thaliana* plants were inoculated with bacterial suspensions (OD_{600} = 0.0001 in 10 mM $MgCl_2$) of *Pst* DC3000 by syringe infiltration. To quantify bacterial growth, leaf discs were collected from the leaves at 1, 2, and 3 days after inoculation. The leaf disks were incubated at 28°C for 2 days and bacterial colonies were counted as described previously (58).

Measurement of Phenolics and Glucosinolates

Leaves from 3- to 4-week-old plants treated with mock or *B. cinerea* were lyophilized and used for extraction. Samples were incubated overnight in darkness at 4°C in 0.5 ml of 80% (v/v) methanol (MeOH), macerated with a pestle, and centrifuged at 15,000 *g* for 5 min. The supernatant was dried and resuspended in 0.1 ml of 80% MeOH. Aliquots (20 µl) were analyzed by HPLC (Dionex, Switzerland). Absorbance spectra were recorded with a PDA-100 photodiode array detector (Dionex, Switzerland). Data integration analysis was conducted using Chromeoleon software (version 6.8, Dionex, Switzerland). The peak height was quantified at 280 nm. Chromatographic conditions were: OD-2 Hypersil 100-5 C_{18} column (5 µm, 2 X 250 mm, Thermo Scientific, Switzerland); flow rate 1.00 ml min^{-1}; gradient (step, time, %A over B) 1, 25 min, 10-25%; 2, 10 min, 25-70%; 3, 5 min, 70-100%; and 4, 10 min, 100-10%). Solvent A was Acetonitrile and solvent B was H_2O, 0.1% (v/v) H_3PO_4. For glucosinolate measurement, leaves from 3- to 4-week-old plants treated with mock or *A. brassicicola* were lyophilized, extracted with 70% MeOH (v/v), and analyzed by HPLC as previously described (59).

Supplementary Table 1. List of primers used in this study

Purpose	Name	Primer sequence (5'-3')
Knockout mutant isolation	LP1(RT-F)	ATGTTAGGACGAGATGAAGATC
	RP1(RT-R)	TTGAGAAGTCATGCACTGATAC
	LP2(RT-F)	CATTCCCTATGCAATTTCTCA
	RP2(RT-R)	CCTTCTTTGGAAGTTGAGGA
qRT-PCR	ABCG34-F	CCGGGATCGAATGATCTCTA
	ABCG34-R	CGAGGAACAATACAGCAGCA
	Actin7-F	AATGGTGAAGGCTGGTTTTG
	Actin7-R	TGCCTCTGTGAGTAGAACTG
	ABCG39-F	CCTTACCTGCTTGGCTTCTG
	ABCG39-R	AAGGGCCATCTGATTCACAC
	Tubulin8-F	TCGATTCGACGGGAAGATAC
	Tubulin8-R	CGGACCGGATCTGACACTAT
	Tubulin8-Ksk-1-F	GCCGAGCACGGGATCGAT
qPCR	CG9	GCATGTCCGCTCACCAATATC
	CG10	GCCTGGGATCTTGGAATGC
	iASK1	CTTATCGGATTTCTCTATGTTTGGC
	iASK2	GAGCTCCTGTTTATTTAACTTGTACATACC

References:

1. Zhou N, Tootlea TL, Glazebrook J (1999) *Arabidopsis PAD3*, a gene required for camalexin biosynthesis, encodes a putative cytochrome P450 monooxygenase. *The Plant Cell* 11: 2419-2428.
2. Mengiste T, Chen X, Salmeron JM, Dietrich RA (2003) The *BOS1* gene encodes

an R2R3MYB transcription factor protein that is required for biotic and abiotic stress responses in *Arabidopsis*. *The Plant Cell* 15: 2551–2565.

3. Grubb CD, Gross HB, Chen DL, Abel S (2002) Identification of *Arabidopsis* mutants with altered glucosinolate profiles based on isothiocyanate bioactivity. *Plant Science* 162: 143–152.